

UNCLASSIFIED

AD NUMBER

AD482359

LIMITATION CHANGES

TO:

Approved for public release; distribution is unlimited.

FROM:

Distribution authorized to U.S. Gov't. agencies and their contractors;
Administrative/Operational Use; MAR 1966. Other requests shall be referred to Air Force Materials Lab., Wright-Patterson AFB, OH 45433.

AUTHORITY

WL ltr 21 Mar 1989

THIS PAGE IS UNCLASSIFIED

482359

AFML-TR-65-2
Part II, Volume V

Orc

**TERNARY PHASE EQUILIBRIA IN TRANSITION METAL-
BORON-CARBON-SILICON SYSTEMS**

**Part II. Ternary Systems
Volume V. Ti-Hf-B System**

**Y. A. Chang
Aerojet-General Corporation**

FILE COPY

**TECHNICAL REPORT NO. AFML-TR-65-2, Part II, Volume V
March 1966**

This document is subject to special export controls and each transmittal to foreign governments or foreign nationals may be made only with prior approval of Metals and Ceramics Division, Air Force Materials Laboratory, Wright-Patterson Air Force Base, Ohio.

lm

REC'D
MAY 25 1966
RECORDED

A

**Air Force Materials Laboratory
Research and Technology Division
Air Force Systems Command
Wright-Patterson Air Force Base, Ohio**

33326

NOTICES

When Government drawings, specifications, or other data are used for any purpose other than in connection with a definitely related Government procurement operation, the United States Government thereby incurs no responsibility nor any obligation whatsoever; and the fact that the Government may have formulated, furnished, or in any way supplied the said drawings, specifications, or other data, is not to be regarded by implication or otherwise as in any manner licensing the holder or any other person or corporation, or conveying any rights or permission to manufacture, use, or sell any patented invention that may in any way be related thereto.



Copies of this report should not be returned to the Research and Technology Division unless return is required by security considerations, contractual obligations, or notice on a specific document.

⑱ AFML ^⑲ TR-65-2 - Pt-2 - Vol-5
Part II, Volume V

① TERNARY PHASE EQUILIBRIA IN TRANSITION METAL-
BORON-CARBON-SILICON SYSTEMS .

Part II. Ternary Systems .
Volume V. Ti-Hf-B System .

② Documentary rept.,

⑩ Y.A. Chang .

⑪ Mar 66,

⑬ AF-7350

⑫ 51 p.

⑭ 735001

⑮ AF/33(615)-1249

This document is subject to special export controls and each transmittal to foreign governments or foreign nationals may be made only with prior approval of Metals and Ceramics Division, Air Force Materials Laboratory, Wright-Patterson AFB, Ohio.

(400042)

1473
aer

FOREWORD

The work described in this report has been carried out at the Materials Research Laboratory, Aerojet-General Corporation, Sacramento, California, under USAF Contract No. AF 33(615)-1249. The contract was initiated under Project No. 7350, Task No. 735001, and was administered under the direction of the Air Force Materials Laboratory, Research and Technology Division, with Captain R.A. Peterson acting as Project Engineer, and Dr. E. Rudy, Aerojet-General Corporation, as Principal Investigator. Professor Dr. Hans Nowotny, University of Vienna, served as consultant to the project.

The project, which includes the experimental and theoretical investigation of selected ternary systems in the system classes Me_1-Me_2-C , $Me-B-C$, Me_1-Me_2-B , $Me-Si-B$, and $Me-Si-C$, was initiated on 1 January 1964. The investigation of selected binary metal-carbon and metal-boron systems was performed as a subtask to the work on the ternary diagrams.

The author is indebted to Dr. E. Rudy for his help in the interpretation of the experimental results. He also wishes to thank E. Spencer for sample preparations, J. Hoffman for Metallographic preparations, R. Cobb for X-ray exposure, D.P. Harmon for many informal discussions, and Dr. A.J. Stosick for technically proofreading the manuscript.

Chemical analyses of the alloys was carried out under the supervision of W. E. Trahan, Metals and Plastics Chemical Testing Laboratory of Aerojet-General Corporation. Mr. R. Cristoni prepared the illustrations and Mrs. J. Weidner typed the report.

The manuscript of this report was released by the author in March 1966 for publication as a RTD Technical Report.

Other reports issued under USAF Contract AF 33(615)-1249 have included:

Part I. Related Binaries

Volume I. Mo-C Systems

Volume II. Ti-C and Zr-C Systems

Volume III. Mo-B and W-B Systems

Volume IV. Hf-C System

Volume V. Ta-C System. Partial Investigation the Systems V-C and Nb-C

Volume VI. W-C System, Supplemental Information on the Mo-C System

Volume VII. Ti-B System

Volume VIII. Zr-B System

Volume IX. Hf-B System

FOREWORD (Cont'd)

Part II. Ternary Systems

Volume I. Ta-Hf-C System

Volume II. Ti-Ta-C System

Volume III. Zr-Ta-C System

Volume IV. Ti-Zr-C, Ti-Hf-C and Zr-Hf-C System.

Part III. Special Experimental Techniques

Volume I. High Temperature Differential Thermal
Analysis

Part IV. Thermochemical Calculations

Volume I. Thermodynamic Properties of Group IV, V,
and VI Binary Transition Metal Carbides.

This technical report has been reviewed and is approved.



W. G. RAMKE
Chief, Ceramics and Graphite Branch
Metals and Ceramics Division
Air Force Materials Laboratory

ABSTRACT

A complete phase diagram for the ternary alloy system titanium-hafnium-boron from 1000°C through the melting ranges of the diborides was established on the basis of X-ray, melting point and metallographic studies. The outstanding features of the system are that both the metal diborides and monoborides form continuous solid solutions with respect to metal exchange.

From the distribution of the tie-lines in the metal monoboride two-phase field, the Gibbs free energy difference between the titanium monoboride and hafnium monoboride was derived.

TABLE OF CONTENTS

	PAGE
I. INTRODUCTION AND SUMMARY.	1
A. Introduction	1
B. Summary	2
1. Binary Systems	2
2. Constitution Diagram Titanium-Hafnium Boron	2
II. LITERATURE REVIEW	6
A. Boundary Systems	6
B. Titanium-Hafnium Boron	9
III. EXPERIMENTAL PROGRAM.	9
A. Experimental Procedures	9
1. Starting Materials	9
2. Alloy Preparation and Heat Treatment	13
3. Melting Points	17
4. Differential Thermal Analysis	17
5. Metallography	18
6. X-Ray Analysis	18
7. Chemical Analysis	18
B. Results	19
1. Titanium-Hafnium	19
2. Titanium-Hafnium Boron	23
IV. DISCUSSION	42
A. Phase Equilibria	42
B. Application	49
References	50

ILLUSTRATIONS

FIGURE		PAGE
1	Tentative Phase Diagram Titanium-Hafnium	3
2	Constitution Diagram Titanium-Hafnium-Boron	4
3	Ti-Hf-B. Isopleth at a 40 Atomic % Boron Composition	7
4	Constitution Diagram Titanium-Hafnium (E. T. Hayes and D.K. Deardorff,)	8
5	Constitution Diagram Titanium-Boron (E. Rudy and St. Windisch, 1965)	10
6	Constitution Diagram Hafnium-Boron (E. Rudy and St. Windisch, 1965)	11
7	Ti-Hf-B: Location of Melting Point Samples	15
8	Ti-Hf-B: Location of Solid State Samples at 1400°C.	16
9	Ti-Hf-B: Location of Metallographic Samples.	16
10	The Lattice Parameters of Titanium-Hafnium Alloys.	20
11	DTA-Thermogram of a Ti-Hf (60/40) Alloy	21
12	DTA-Thermogram of a Ti-Hf (10/90) Alloy.	22
13	Phase Equilibria of Ti-Hf-B System at 1400°C.	24
14	Lattice Parameters of the Diboride Solid Solutions.	25
15	Lattice Parameters of the Monoboride Solid Solutions.	27
16	Micrograph of an Arc-Melted Ti-Hf-B (75/25/5) Alloy.	28
17	Micrograph of an Arc-Melted Ti-Hf-B (55/20/25) Alloy.	28
18	Micrograph of an Arc-Melted Ti-Hf-B (20/70/10) Alloy.	29
19	Micrograph of an Arc-Melted Ti-Hf-B (10/80/10) Alloy.	29
20	Compositions (Top) and Temperatures of the Metal-Rich Eutectic Trough	30 30
21	Compositions (Top) and the Peritectic Temperatures of the Monoboride Solid Solutions	32
22	Micrograph of an Arc-Melted Ti-Hf-B (50/0/50).	32

ILLUSTRATIONS (Continued)

FIGURE		PAGE
23	Micrograph of an Arc-Melted Ti-Hf-B (45/5/50).	33
24	Micrograph of an Arc-Melted Ti-Hf-B (5/45/50).	33
25	Composition (Top) and the Melting Temperatures of Diboride Solid Solutions	34
26	Micrograph of a Ti-Hf-B (16.7/16.6/66.7) Alloy	36
27	Liquidus Projections in the Titanium-Hafnium-Boron System	37
28-35	Ti-Hf-B. Isothermal Sections from 1400°C to 3300°C . . .	38-41
36	Calculated Phase Equilibria in Ti-Hf-B System at 1400°C .	47

TABLES

TABLE		PAGE
1	Lattice Parameters of Titanium-Hafnium Alloys	21

I. INTRODUCTION AND SUMMARY

A. INTRODUCTION

Due to the good oxidation-resistant properties of hafnium diboride, it is considered for use as a major component in composite systems with other materials. Consequently, it is important to have information concerning the interactions between the various diborides themselves, as well as between the diborides and the elemental metals and boron. Unfortunately, little phase-equilibrium data existed in the literature for systems such as the titanium-hafnium-boron system. The purpose of the present investigation is to establish the phase relationships in this technologically important alloy system from 1400°C through the melting range of the diborides.

Phase equilibria of binary and ternary alloy systems, in principle, can be predicted from chemical thermodynamics. However, the lack of pertinent data often makes such predictions impossible. Moreover, the Gibbs free energy of formation of a hypothetical binary alloy which affects the solubility of this alloy in another real binary alloy cannot be obtained using conventional thermochemical methods since this pure hypothetical binary alloy is unstable. However, in a converse way once a ternary phase diagram is established experimentally, one can then derive the relative free energy values for the various phases. One can, for example, derive the difference in Gibbs free energy of two binary alloys, even though one of the binaries cannot exist as a pure phase. In a similar way, one can derive the decomposition energy of a hypothetical binary phase to two other phases by applying the methods developed by Rudy⁽¹⁾. This information, together with other thermodynamic data obtained utilizing conventional thermochemical means, can be used to predict phase equilibria of systems which have not been investigated experimentally.

B. SUMMARY

the ternary alloy system titanium-hafnium-boron and the binary titanium-hafnium system were investigated by X-ray, metallographic, melting point and DTA techniques. The melting-point samples of the ternary alloys were prepared exclusively by hot-pressing. After hot-pressing, only the 50 atomic % boron alloys were heat-treated at 1450°C under a vacuum of 5×10^{-6} mm Hg for 300 hours before melting point determination in the hope that the solid solution formation would be complete. The post-melting samples were heat-treated at 1400°C under a vacuum of 5×10^{-6} mm Hg for solid state investigation. For metallographic examinations, either the melting samples or arc-melted samples were used.

The hcp-bcc transformation temperatures and the melting points of five arc-melted titanium-hafnium alloys were determined by DTA-method.

1. Binary Systems

The binary systems titanium-boron and hafnium-boron have been recently re-investigated by Rudy and Windisch^(2,3) and described in previous documentary reports. The metal binary system titanium-hafnium (Figure 1) was investigated only superficially in the present study. The hcp-bcc transformation temperatures as well as the melting temperatures obtained are in good agreement with those reported by Hayes and Deardorff⁽⁴⁾. Although not experimentally established, a minimum must exist in the liquidus and solidus curves. The congruent melting composition is indicated at about 10 atomic % hafnium.

2. Constitution Diagram Titanium-Hafnium-Boron

The constitution diagram titanium-hafnium-boron is presented in Figure 2. The main features of this system are described in the following:

a. The Hexagonal (C-32) Diboride Phase (6)

Titanium diboride ($a = 3.025 \text{ \AA}$ and $c = 3.226 \text{ \AA}$) and hafnium diboride* ($a = 3.140 \text{ \AA}$ and $c = 3.471 \text{ \AA}$) form a continuous series

*See Section III for zirconium content

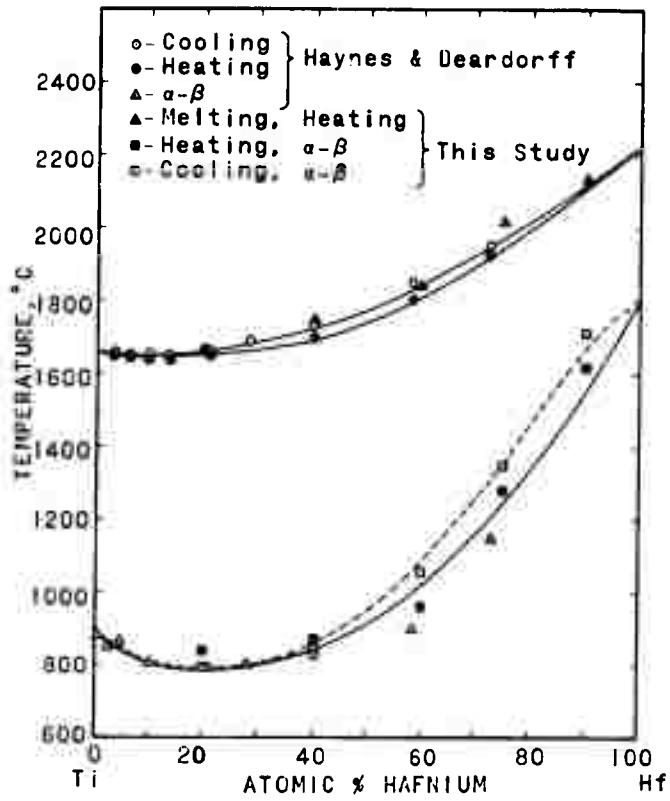


Figure 1. Tentative Phase Diagram Titanium-Hafnium

of solid solutions. Both the lattice parameters a and c for the solid solutions show slight positive deviations from a linear relationship with composition.

b. The Orthorhombic (B27) Monoboride Phase (γ)

Titanium monoboride ($a = 6.14 \text{ \AA}$, $b = 3.06 \text{ \AA}$ and $c = 4.57 \text{ \AA}$) and hafnium monoboride ($a = 6.521 \text{ \AA}$, $b = 3.221 \text{ \AA}$ and $c = 4.921 \text{ \AA}$) also form a continuous series of solid solutions. Within the scatter of data the lattice parameters a and b increase linearly with hafnium exchange, while the parameter c shows a slight positive deviation from a linear relationship with composition.

The formation of the hafnium-rich monoboride solid solutions at 50 atomic % boron was never complete even after long-time heat treatment, presumably due to a nucleation problem⁽³⁾. However, X-ray and metallographic examinations of the 25 atomic % boron alloys showed only the monoboride and metal phases. Moreover, the lattice parameters of the monoboride phase present in the 25 atomic % boron alloys vary smoothly with hafnium exchange.

The monoboride solid solutions melt peritectically with a rapid drop of the peritectic temperature from 2190°C at the titanium side to 2100°C which is the peritectic temperature of the pure hafnium monoboride.

c. Metal-Rich and Boron-Rich Equilibria

There is no four-phase reaction in the titanium-hafnium-boron system. The metal-rich eutectic trough extends from the titanium-side with 7 atomic % boron to the hafnium side with 13 atomic % boron. The eutectic temperatures increase smoothly starting from the titanium side, and increase sharply when the pure hafnium monoboride-hafnium eutectic is approached.

Due to the existence of a hcp (α) - bcc (β) two-phase field in the metal binary system, a three-phase field between the α -, β - and γ -phases is formed in the temperature region from the α - β -transformation temperature of pure titanium to that of pure hafnium.

An isopleth at a 40 atomic % boron composition, which shows the phase reactions in the metal-rich solutions, is shown in Figure 3.

The boron-rich eutectic trough between the diboride solid solutions and boron as shown in Figure 2 was estimated to be consistent with the boundary binary systems.

II. LITERATURE REVIEW

A. BOUNDARY SYSTEMS

The titanium-hafnium system as shown in Figure 4, exhibited complete solubility between both the hcp (α) and bcc (β) forms, was established by Hayes and Deardorff⁽⁴⁾ using a DTA technique and melting point determinations. As pointed out by Hayes and Deardorff, there must exist a two-phase field which separates the α - and β -phase. However, due to the scatter of data obtained from the cooling and heating curves, the α - β -transformation temperatures were shown as a single line.

The literature data concerning the phase relationships of the titanium-boron and hafnium-boron systems up to 1953 have been summarized and evaluated by Hansen⁽⁵⁾. According to Hansen, there exist four intermediate phases, Ti_2B , TiB , TiB_2 , and Ti_2B_3 in the titanium-boron system, and only two intermediate phases, HfB and HfB_2 , in the hafnium boron system. The phase equilibria of the titanium-boron system in the melting range were uncertain, while those of the hafnium-boron system were not even studied with the exception that the melting point of HfB_2 was reported to be $3250 \pm 100^\circ C$.

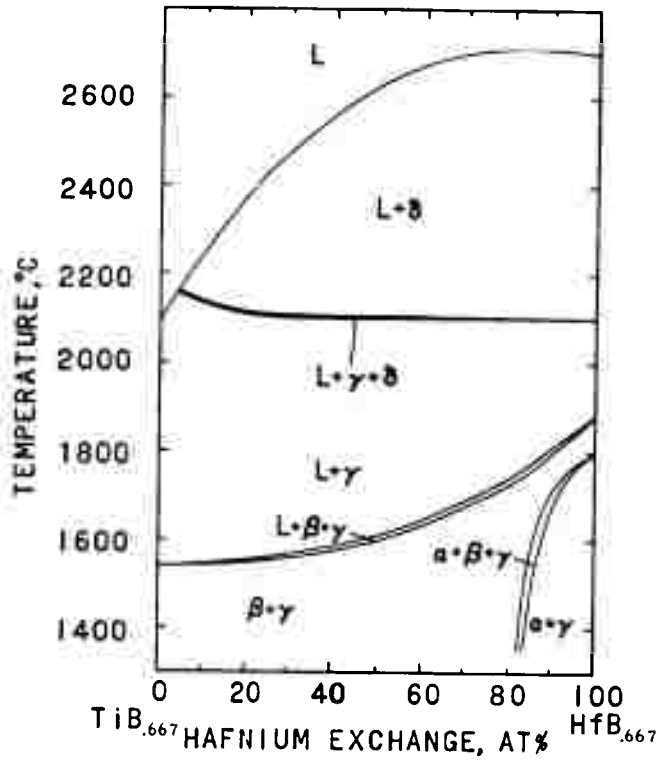


Figure 3. Ti-Hf-B: Isopleth at a 40 Atomic % Boron Composition .

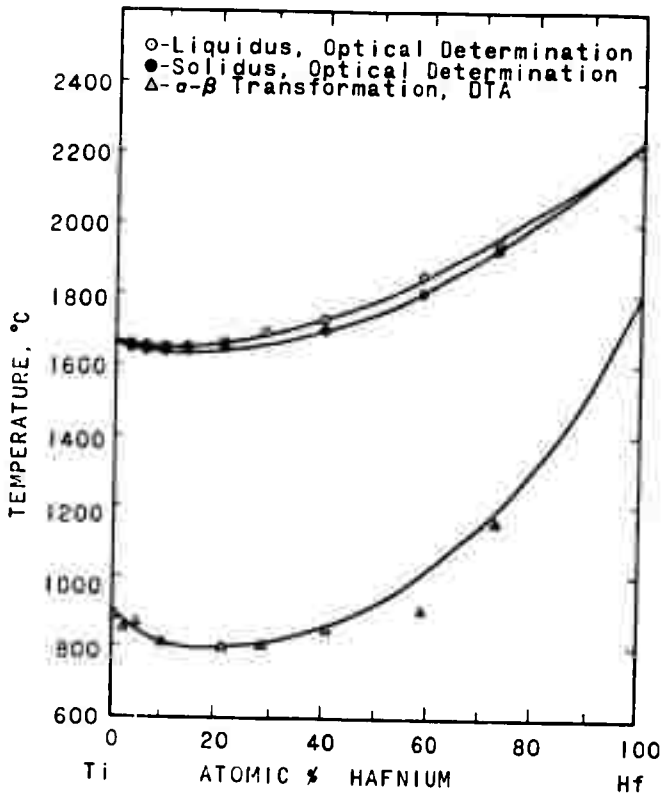


Figure 4. Constitution Diagram Titanium-Hafnium.
 (E.T. Hayes and D.K. Deardorff, 196)

In view of the scarcity of data and partially conflicting data concerning the phase relationships of the titanium-boron and hafnium-boron systems which existed in the literature, both systems were recently reinvestigated by Rudy and Windisch^(2, 3) of this laboratory.

In contrast to previous findings, only two intermediate phases — a monoboride with an orthorhombic structure (B27), and a diboride with a hexagonal structure (C32) — were found to exist in both systems by Rudy and Windisch as shown in Figures 5 and 6. The monoboride melts peritectically while the diboride melts congruently.

B. TITANIUM-HAFNIUM-BORON

Relatively little information concerning the phase relationships of the titanium-hafnium-boron system exist in the literature. Post, Glaser, and Moskowitz⁽⁶⁾ found that the titanium and hafnium diborides are completely soluble in each other. The lattice parameters of one $(\text{Ti, Hf})\text{B}_2$ with 50 Mole % HfB_2 determined by Post, et.al. were $a = 3.085 \text{ \AA}$ and $c = 3.368 \text{ \AA}$. By heating a Ti- HfB_2 mixture to 1000°C , Antony and Cummings⁽⁷⁾ found the presence of HfB_2 as well as TiB by means of X-ray.

III. EXPERIMENTAL PROGRAM

A. EXPERIMENTAL PROCEDURES

1. Starting Materials

The ternary alloys used in this investigation were prepared from titanium diboride, hafnium diboride, titanium and hafnium metal powders and elemental boron powder.

The metal diborides were prepared by directly reacting the elemental metal and boron powders. The titanium metal powder used was

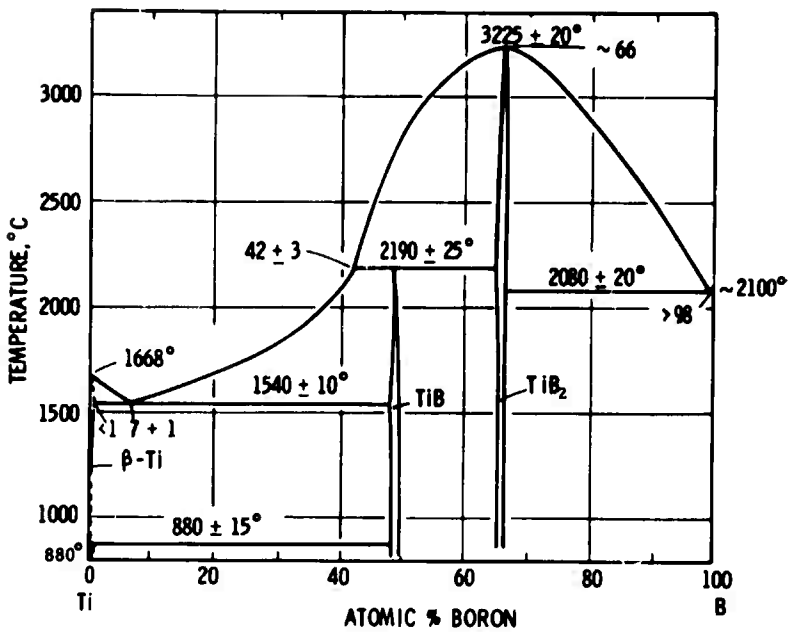


Figure 5. Constitution Diagram Titanium-Boron .
 (E. Rudy and St. Windisch, 1965)

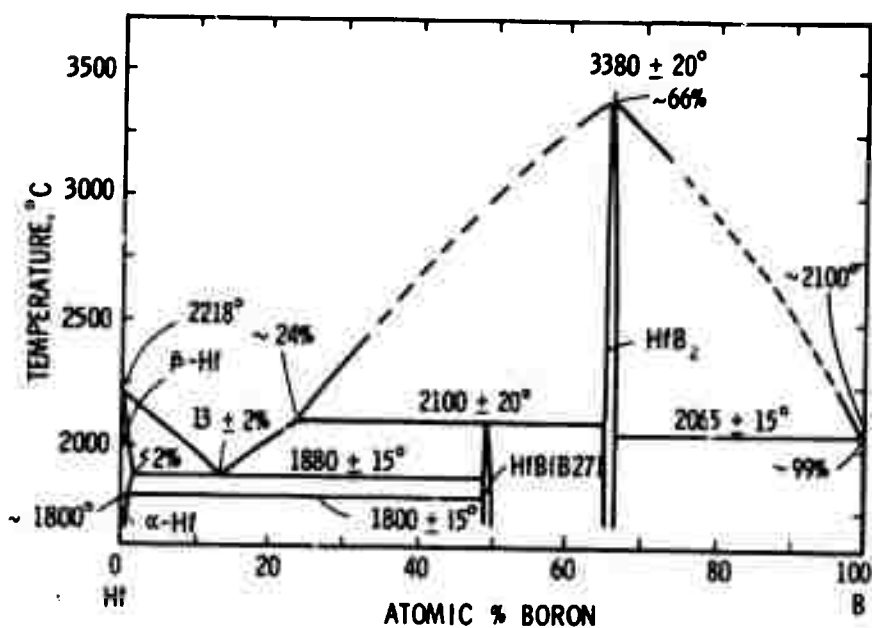


Figure 6. Constitution Diagram Hafnium-Boron.
(E. Rudy and St. Windisch, 1965)

purchased from Var-Lac-Old Chemical Company, New York, and had the following analysis: 99.8% Ti, 0.13% C, 0.15% H, 0.005% N, 0.05% Fe, and 0.12% Cl. The lattice parameters of this starting material determined from a powder pattern using Cu-K α radiation were $a = 2.950 \text{ \AA}$ and $c = 4.683 \text{ \AA}$. The boron powder, purchased from United Mineral and Chemical Corporation, had the following analysis: 99.55% B, 0.25% Fe and 0.08% C. The resulting titanium diboride having stoichiometric composition was comminuted in hard metal lined ball mills. The carbon concentration in the titanium diboride was 0.35% and the lattice parameters of this diboride were $a = 3.025 \text{ \AA}$ and $c = 3.226 \text{ \AA}$.

The hafnium powder used to make the hafnium diboride was purchased from Wah Chang Corporation, Albany, Oregon, and had the following analysis in ppm: Al-44, B<.2, C-<60, Nb-<100, Cd-<1, Co-<5, Cr-<10, Cu-<40, Fe-99, H-45, Mg-<10, Mn-<10, Mo-<10, N-<200, Ni-<10, O-660, Pb-<5, Si-<40, Sn-<10, Ta-<200, Ti-<39, V-<5, W-<20, and Zr-2500. The resulting hafnium diboride had 10.15% B and 0.17% C. The lattice parameters of this hafnium diboride were $a = 3.140 \text{ \AA}$ and $c = 3.471 \text{ \AA}$.

For hafnium-rich alloys, hafnium hydride was used instead of hafnium metal powder, in order to make alloys of desired compositions. The hafnium hydride was also purchased from Wah Chang Corporation, Albany, Oregon. The impurities present in this material in ppm were: Al-80, B-<0.2, C-50, Nb-100, Cd-<1, Co-<5, Cr-<10, Cu-60, Fe-190, Mg-250, Mn-<10, Mo-<10, N-20, Ni-<10, Pb-<5, Si-<40, Sn-<10, Ta-<200, Ti-75, N-<5, W-<20, O-<330, and Zr-1350. The hydrogen content was 0.92%.

The binary titanium-hafnium alloys were prepared from titanium bar of high purity and hafnium sponge since metals in the form of

sponge have less surface area than in the powder form and consequently less chance to form metal oxides. The titanium bar, purchased from Foote Mineral Company had the following analysis in percentage: Si-<0.001, Al-<0.005, Mg-<.001, Mn-<0.005, Pb-<0.001, Cr-<0.001, Fe-<0.001, Ni-<0.001, Mo-<.001, Ca-<.005, Cu-<.003, Sn-<.001, Zr-<.015. The hafnium sponge was again purchased from Wah Chang Corporation, Albany, Oregon. The impurities in the sponge in ppm were: Al-94, B-<0.2, Cd-<1, Co-<5, Cr-<10, Cu-<40, Fe-185, Cl-100, Mg-450, Mn-<10, Mo-<10, N-30, Ni-<10, O-680, Pb-<5, Si-<40, Sn-<10, Ti-250, V-<5, W-<20, U-<0.5, and Zr-2100.

2. Alloy Preparation and Heat Treatment

In the present study, the cylindrical melting point samples of approximately 10 mm in diameter and 30 mm in length with a rectangular or cylindrical groove in the center were prepared by hot-pressing of well-mixed powder mixtures in graphite dies. Before determining the melting points of these alloys, the hot-pressed samples were ground on sand paper to remove any minute surface contamination of carbides. A small hole of about 1 mm diameter, drilled in the center portion of the sample, served as the black body cavity for the temperature measurements.

For alloys in the monoboride region, the melting samples, after removing any surface contamination of carbide, were heat-treated at 1450°C under a vacuum of $<5 \times 10^{-6}$ mm for 300 hours before melting point determinations in the hope that the formation of solid solutions of titanium and hafnium monoboride would be complete. Unfortunately, the reaction rate for the formation of the monoboride solid solution in the hafnium-rich side was so slow that solid solution was never completely formed. The problem concerning the solid solution formation of the monoboride will be discussed in later sections.

The samples for solid state investigation, obtained from the post-melting point samples, were heat treated at 1400°C under a vacuum of $<5 \times 10^{-6}$ mm for 92 hours. All alloys attained equilibrium as evidenced by X-ray investigation with the exception of the hafnium-rich monoboride alloys.

Additional alloys in the monoboride region were also made from the elemental metal, metal hydride and boron powder instead of the diborides as the starting materials. It was believed that the monoboride would be formed more readily from the elemental metals and boron than from the diboride and metal. However, the hafnium-rich monoboride alloys prepared in this manner followed by long time heat treatment at 1400°C under a vacuum of $<1 \times 10^{-5}$ mm Hg again did not attain equilibrium. This statement does not mean that the monoboride does not form readily from the elemental powders; rather it suggests that the primary reaction product was diboride whose sluggish reaction with metal prevents any formation of the monoboride phase.

The existence of a series of continuous solid solutions between titanium- and hafnium monoborides was proved by analyzing the two-phase alloys having 25 atomic % boron using X-ray and metallographic techniques. Since the boron concentration of the peritectic point in both the titanium- and hafnium-boron system is higher than 25 atomic % boron, the primary phase formed when cooling an alloy from its liquid phase is the monoboride phase rather than diboride. The experimental results and the analysis of data will be presented in detail in later sections.

Whenever the melting point samples were not sufficiently dense, they were arc melted in a non-consumable tungsten electrode melting furnace. The samples were then examined both by X-ray and metallographic technique.

The locations of the melting point samples, the solid state samples at 1400°C and the metallographic samples are shown in Figures 7 through 9.

Since the lattice parameters of the binary titanium-hafnium alloys were not available in the literature, five metal alloys were prepared from titanium bar and hafnium sponge by arc melting. After arc melting six times, these alloys were heat-treated at 1200°C under a vacuum of $<5 \times 10^{-5}$ mm Hg for two hours. Fine powders filed from these alloys were stress annealed at 800°C for one hour under a vacuum of $<5 \times 10^{-5}$ mm Hg and subsequently X-rayed.

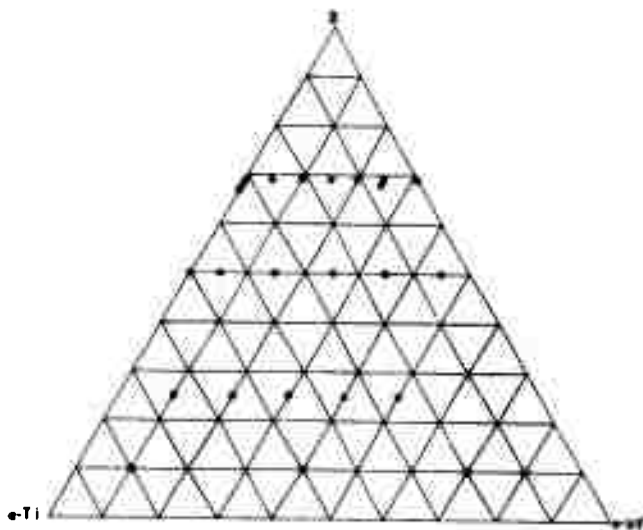


Figure 7. Ti-Hf-B: Location of Melting Point Samples

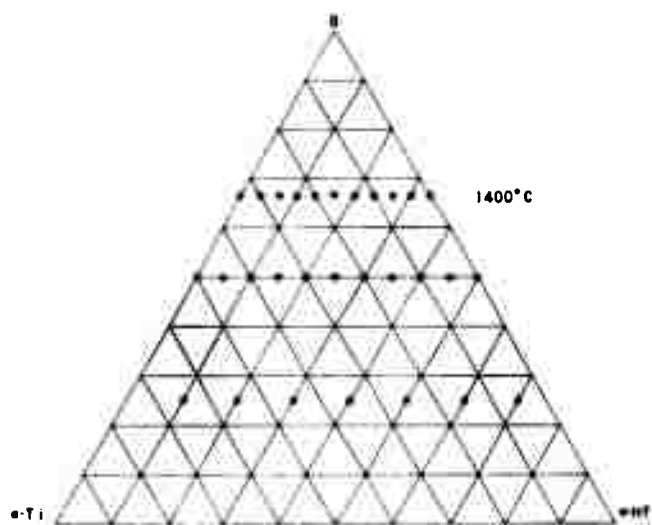


Figure 8. Ti-Hf-B: Location of Solid State Samples at 1400°C.

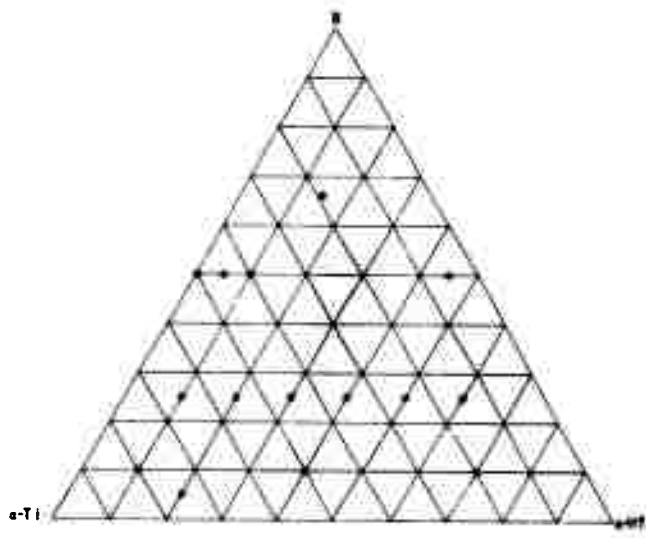


Figure 9. Ti-Hf-B: Location of Metallographic Samples.

3. Melting Points

The melting points of the selected alloys as shown in Figure 7 was determined by the Pirani-technique which has been extensively described previously⁽⁸⁾.

The temperature measurements were carried out with a disappearing filament type micropyrometer, which was calibrated against a certified lamp from the National Bureau of Standards. The temperature was corrected for absorption losses in the quartz window of the melting point apparatus and deviations due to non-black body conditions of the observation hole. The detailed treatment with regard to the temperature correction has been discussed earlier⁽⁸⁾ and will not be repeated here.

To prevent any appreciable loss of boron or metal from the melting samples during the course of the melting point determination, the furnace chamber was pressurized to about 2 1/4 atmospheres with high purity helium after a short vacuum degassing treatment at temperatures below the incipient melting points.

4. Differential Thermal Analysis

Differential thermal analysis has been proven to be one of the useful methods in determining the temperature at which a material undergoes a phase transformation. In the present study, the α - β -transformation and the melting temperatures of five titanium-hafnium alloys were determined by means of the DTA technique.

The details of the DTA-apparatus has been discussed extensively in previous publication^(8, 9) and will not be repeated here.

5. Metallography

The metallographic samples, which had been either a small portion of the molten zone of the melting point sample, or arc melted samples whenever the molten zone of the melting point sample was not sufficiently dense, were mounted in an electrically conductive mixture of diallylphtalate-lucite-copper powder. After coarse grinding on silicon carbide powder (grit sizes varying between 120 and 600), the samples were first polished on microcloth, using a slurry of 0.05 micron alumina and 5% chromic acid solution, and then etched electrolytically in a 10% aqueous oxalic acid solution.

6. X-Ray Analysis

Debye-Scherrer powder diffraction patterns, using Cu-K α radiation, were made of all samples after melting point and solid state investigations, as well as of arc melted samples. To eliminate the film-blackening caused by titanium fluorescence radiation, a cover film which absorbed this soft white radiation was used over the films during the exposure.

7. Chemical Analysis*

The dissolution of alloy powders for boron analysis was achieved by fusion in pre-dried sodium carbonate at 1000°C. The resulting melt was dissolved in water, and excess carbonate removed by barium hydroxide. After removal of the precipitants, boric acid content was determined by differential titration of the boromannitol complex with 10 N NaOH between pH values of 5.3 and 8.5. Depending on the sample material, the consistency of data obtained by this method varied between ± 0.1 and ± 1.0 atomic % boron absolute.

*The chemical analyses were performed under the supervision of Mr. W. E. Trahan, Metals and Plastics Chemical Testing Laboratory of Aerojet-General Corporation.

B. RESULTS

1. Titanium-Hafnium

The lattice parameters of the hcp solid solutions of titanium and hafnium obtained from powder patterns using CuK α radiation are summarized in Table 1, and plotted as a function of composition in Figure 10. The c-parameter increases linearly with concentration from titanium to hafnium, while the a-parameter exhibits a slight negative deviation from a linear relationship. The extrapolated values to pure hafnium (see starting material for zirconium content) are in good agreement with a value presented by Cullity⁽¹⁰⁾, but higher than the values reported by Russell⁽¹¹⁾. The discrepancy is probably due to different amounts of zirconium present. From an analysis of weight losses of the arc-melted alloys, the nominal composition as given in Table 1 should be within ± 1 atomic % of the actual composition.

Typical DTA curves for one titanium-rich and one hafnium-rich alloys are shown in Figures 11 and 12. Since the α - β transformation peaks for the 20 and 40 atomic % Hf alloys are much sharper than alloys with higher hafnium content, it is concluded that the α - β two-phase field on the titanium-rich side must be relatively narrow.

It is noteworthy to point out that the α - β transformation temperatures obtained from the heating curves for the two titanium-rich alloys are higher than those obtained from the cooling curves. The phenomenon is undoubtedly due to a kinetic effect. As the heating and cooling rates approach zero, the two temperatures should cross each other. In any case, the temperature difference obtained from the heating and cooling curves are within the uncertainty of our temperature measurements.

The α - β transformation as well as the melting temperatures of the five titanium-hafnium alloys are shown in Figure 1 (see summary

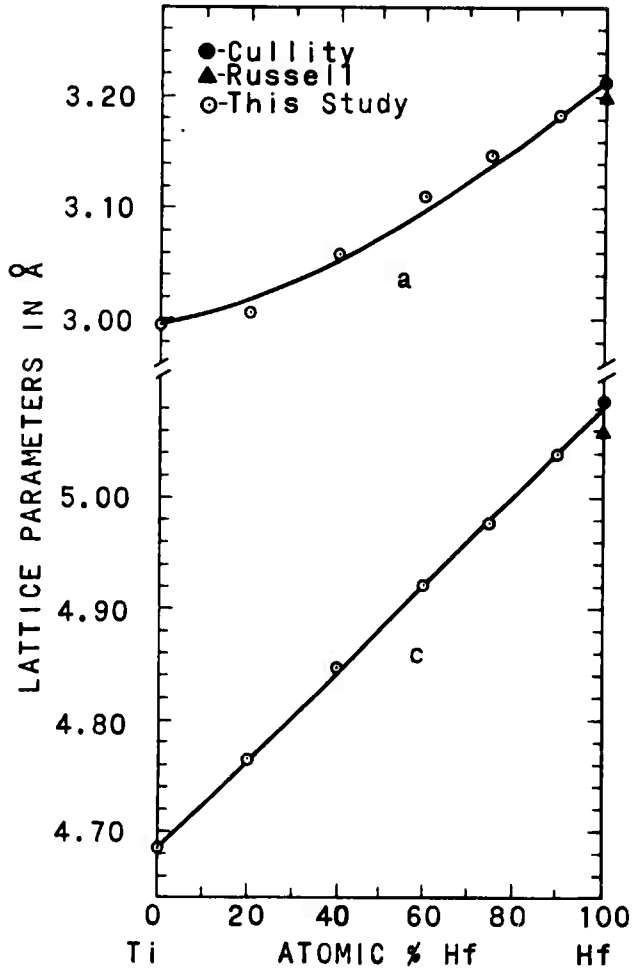


Figure 10. The Lattice Parameters of Titanium-Hafnium Alloys.

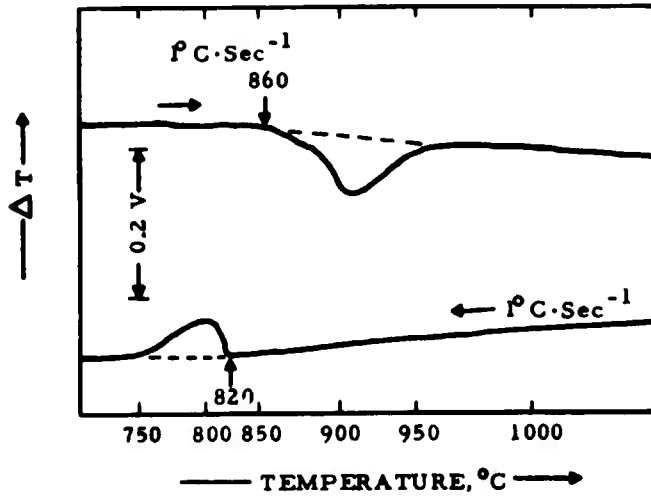


Figure 11. DTA-Thermogram of a Ti-Hf (60/40) Alloy.

Table 1. Lattice Parameters of Titanium-Hafnium Alloys.

Nominal Composition Atomic % Hf	a, Å	c, Å
20	3.006	4.765
40	3.058	4.846
60	3.111	4.922
75	3.146	4.976
90	3.183	5.038

on page 3). One can see from this figure that the data obtained in the present study agree reasonably well with those of Hayes and Deardorff⁽⁴⁾. The liquidus and solidus curves as well as the α - β two-phase boundaries (Figure 1) are drawn based on the data of Hayes and Deardorff and those of the present study.

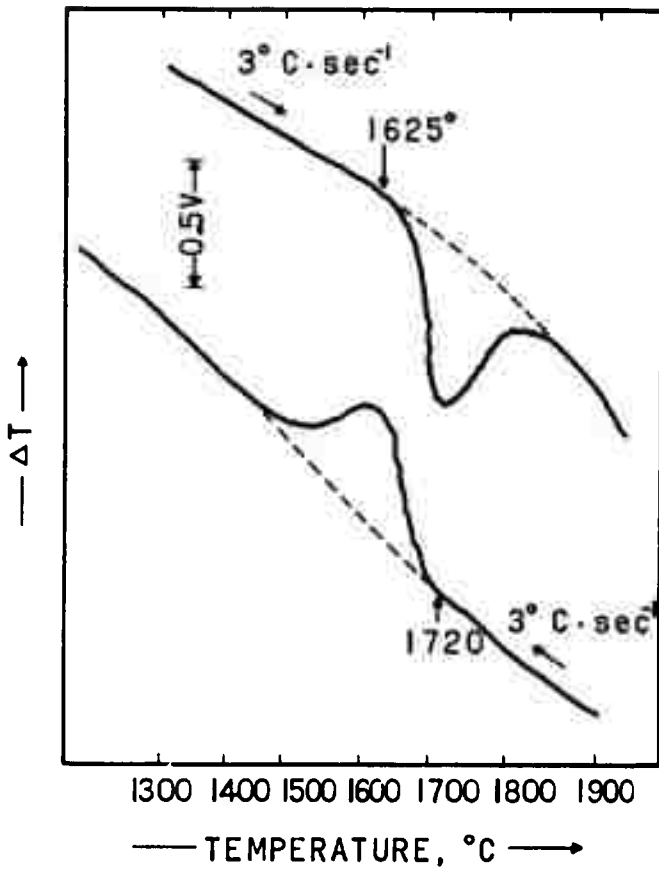


Figure 12. DTA-Thermogram of a Ti-Hf (10/90) Alloy.

2. Titanium-Hafnium-Boron

The phase equilibria of the titanium-hafnium-boron system at 1400°C as determined primarily from X-ray analysis of the heat-treated samples are shown in Figure 13. Titanium diboride and hafnium diboride form a series of continuous solid solutions as evidenced by both X-ray and metallographic examinations. Both the lattice parameters a and c for the diboride solid solutions, as shown in Figure 14, show slight positive deviation from a linear relationship. The values for a 50 mole % HfB_2 alloy obtained by Post, Glaser and Moskowitz⁽⁶⁾ are in good agreement with the results of the present investigations.

The alloys in the monoboride region with hafnium exchange of more than 20 atomic % never attained equilibrium. X-ray analysis of these alloys showed the presence of diboride, monoboride, and metal phases. Since the lattice parameters of the diboride phase present in all these alloys change progressively with increasing hafnium content, the possibility of a three-phase equilibrium between the diboride, monoboride, and metal phases is ruled out.

The existence of a series of continuous solid solution between TiB and HfB is proved by analyzing the 25 atomic % B alloys. Both X-ray and metallographic examination of these alloys revealed only the presence of monoboride and metal phases. From the calculated lattice parameters of the metal phase present in the two-phase alloys and the known lattice parameters of the (Ti-Hf) solid solution (Table 1 and Figure 10), tie lines connecting the two coexisting phases were established as shown in Figure 13. Due to the existence of a α - β two-phase field between the α -(Ti, Hf) and β -(Ti, Hf) solid solutions at 1400°C, a three-phase field, i. e., α -(Ti, Hf)- β -(Ti, Hf)-(Ti, Hf)B is formed.

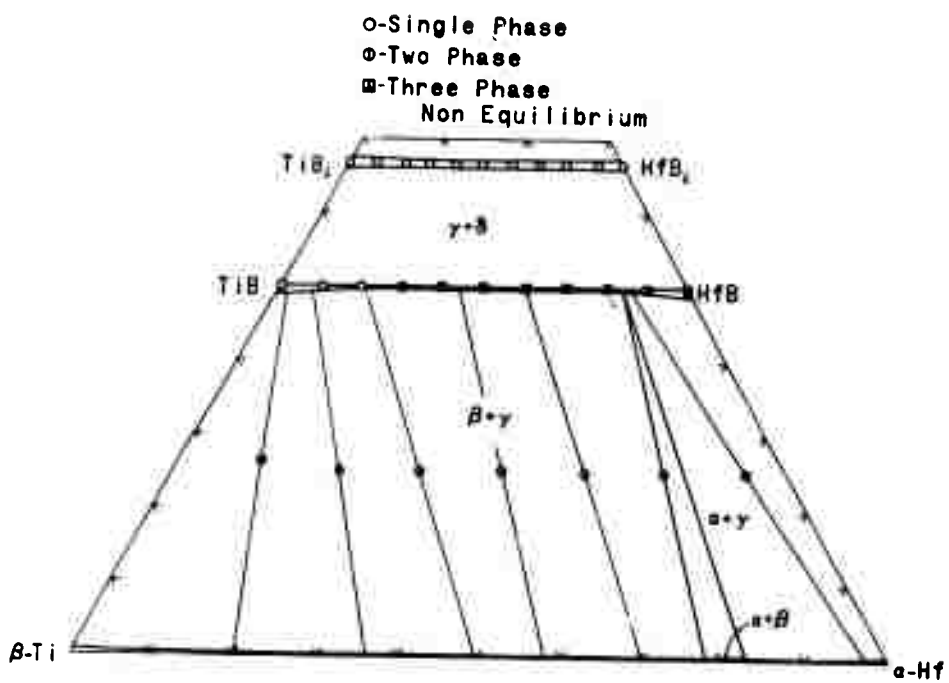


Figure 13. Phase Equilibria of Ti-Hf-B System at 1400°C.

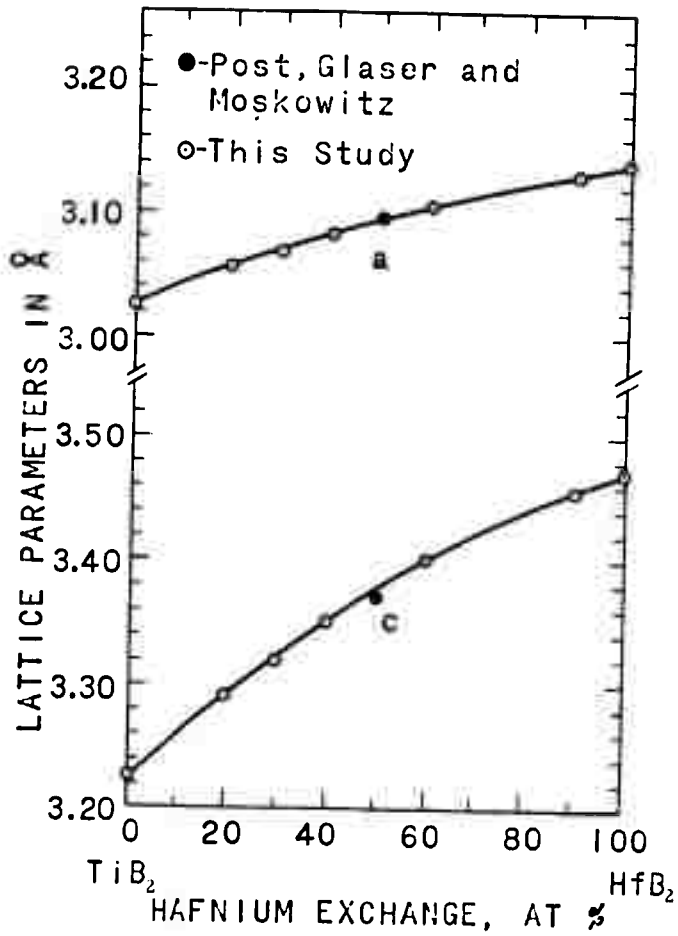


Figure 14. Lattice Parameters of the Diboride Solid Solutions.

The lattice parameters of the monoboride solid solutions obtained from the single-phase alloys (50 atomic % B) as well as from the two-phase alloys (25 atomic % B) are plotted as a function of hafnium exchange as shown in Figure 15. The lattice parameters of TiB obtained in the present investigation agree with those of Decker and Kasper⁽¹²⁾. Within the scatter of our data, the lattice parameters a and b increase linearly with hafnium exchange as shown in Figure 15, while the c-parameter shows a slight positive deviation from a linear relationship. All three lattice parameters join in smoothly with the lattice parameters of HfB as reported by Rudy and Benesovsky⁽¹³⁾.

According to chemical analysis for boron content, the alloy Ti-Hf-B (65/10/25) lost about 1 atomic % metal after a 92 hour heat-treatment in vacuum at 1400°C. Based on this evidence, it is believed the nominal compositions of all the ternary alloys, with the exception of the diboride samples, must be within 1 atomic % of the actual compositions.

The location of the metal-rich eutectic trough extending from the titanium side to the hafnium side was established exclusively by metallographic examinations of alloys having 5, 10, and 25 atomic % boron (see Figure 9 for the compositions of the metallographically examined samples). The micrograph of an arc-melted Ti-Hf-B (75/25/5) alloy as shown in Figure 16 shows the primary crystallization of the metal phase exhibiting the α - β transformation structure and the metal-rich eutectic structure. On the other hand, the micrograph of an arc-melted Ti-Hf-B (55/20/25) alloy as shown in Figure 17 shows the primary crystallization of the monoboride phase and the metal-rich eutectic structure. The micrographs of two alloys: Ti-Hf-B (20/70/10) and Ti-Hf-B (10/80/10) as shown in Figures 18 and 19 exhibit the metal-rich eutectic structures.

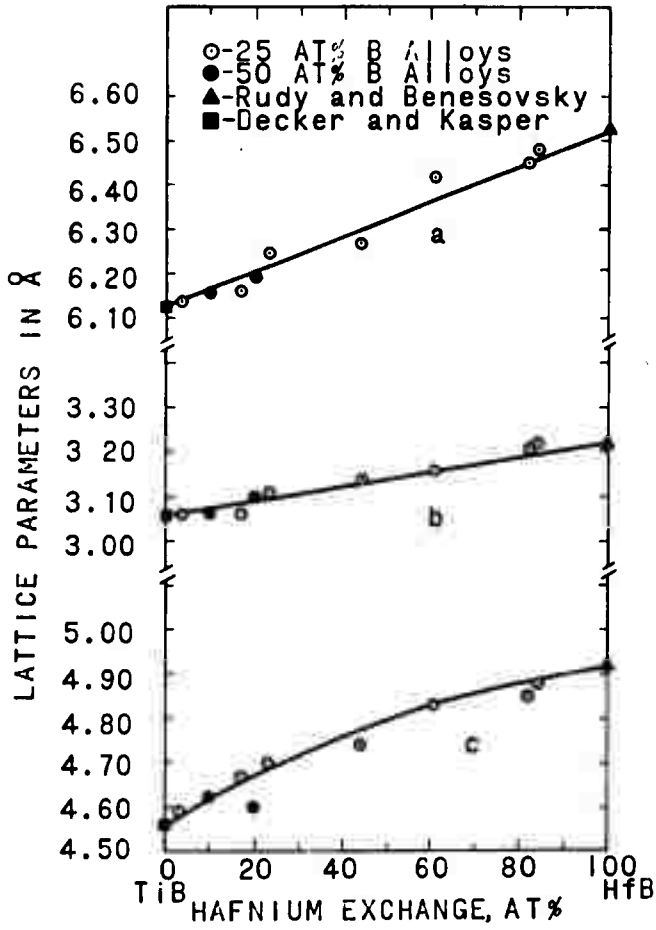


Figure 15. Lattice Parameters of the Monoboride Solid Solutions

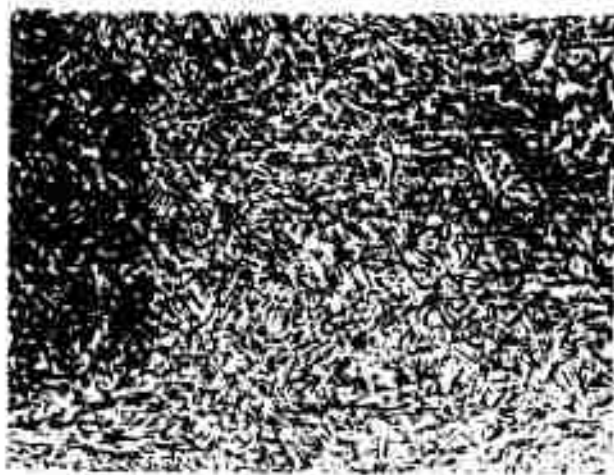


Figure 16. Micrograph of an Arc-Melted Ti-Hf-B (75/25/5) Alloy. X1000

Primary Crystallization of Metal Phase Exhibiting the α - β Transformation Structure and the Metal-Rich Eutectic Structure.



Figure 17. Micrograph of an Arc-Melted Ti-Hf-B (55/20/25) Alloy X100

Primary Crystallization of the Monoboride Phase (Dark) and the Metal-Rich Eutectic Structure.

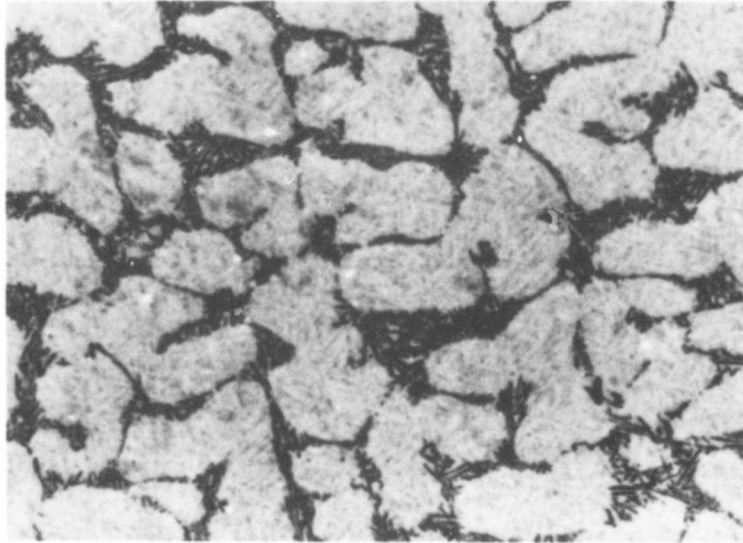


Figure 18. Micrograph of an Arc-Melted Ti-Hf-B (20/70/10) Alloy.

X150

Eutectic Structure.

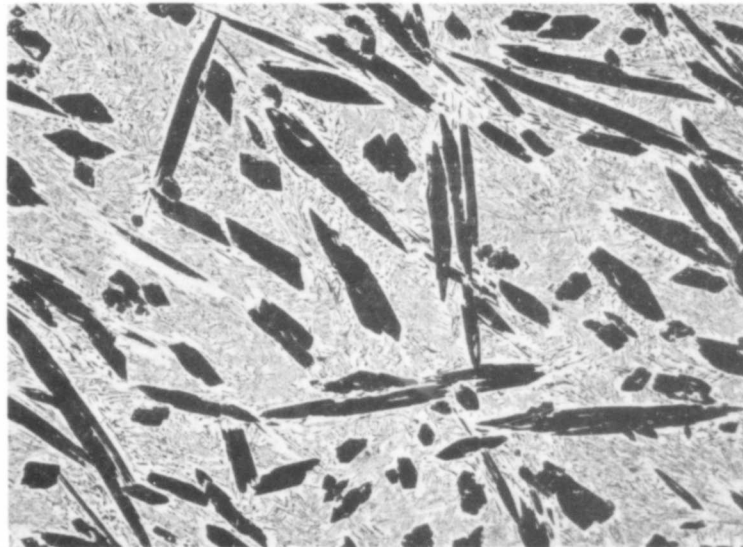


Figure 19. Micrograph of an Arc-Melted Ti-Hf-B (10/80/10) Alloy.

X460

Eutectic Structure.

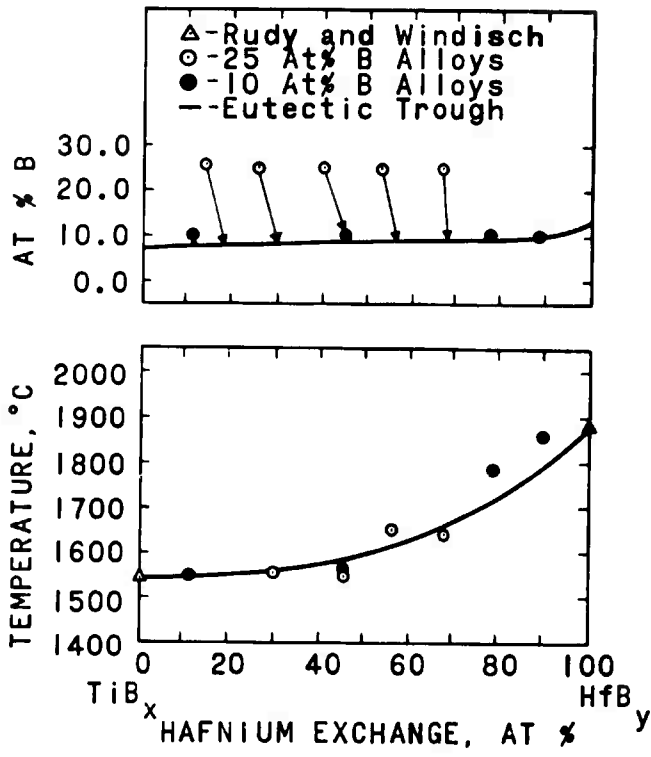


Figure 20. Composition (Top) and Temperature of the Metal-Rich Eutectic Travel.

The incipient melting points as well as the boron content at the metal-rich eutectic trough are plotted as a function of hafnium exchange in Figure 20. The eutectic temperature of the two binary systems: Ti-TiB and Hf-HfB as determined by Rudy and Windisch^(2, 3) are also shown in the figure.

The determination of the peritectic temperatures of the hafnium-rich monoboride solid solutions was difficult since the alloys even after 300 hour heat treatment at 1450°C did not completely reach equilibrium. The measured melting points for the monoboride solid solutions as a function of hafnium exchange are shown in Figure 21. The peritectic temperature of TiB obtained in the present study agrees with that of Rudy and Windisch⁽²⁾. For hafnium-rich monoborides the values of the peritectic temperatures were uncertain and are dotted in Figure 21 to agree with the peritectic temperature of pure hafnium monoboride as determined by Rudy and Windisch⁽³⁾. The peritectic concentrations were estimated based on the binary data and are also dotted in Figure 21. Since the peritectic temperatures of the titanium-rich monoboride solid solutions drop rapidly from 2190°C to 2100°C (which is the peritectic temperature of pure HfB) as shown in Figure 21, one does not expect that the temperature will change drastically toward the hafnium side. The relatively low values of the incipient melting points for the two hafnium-rich monoboride alloys are most probably due to the presence of the unreacted metal-diboride mixture.

The micrographs of two arc-melted titanium-rich monoboride solid solutions which show the peritectic-type of reaction are shown in Figures 22 and 23. On the other hand, a micrograph of an arc-melted hafnium-rich monoboride, Ti-Hf-B (5/45/50) as shown in Figure 24 shows that the

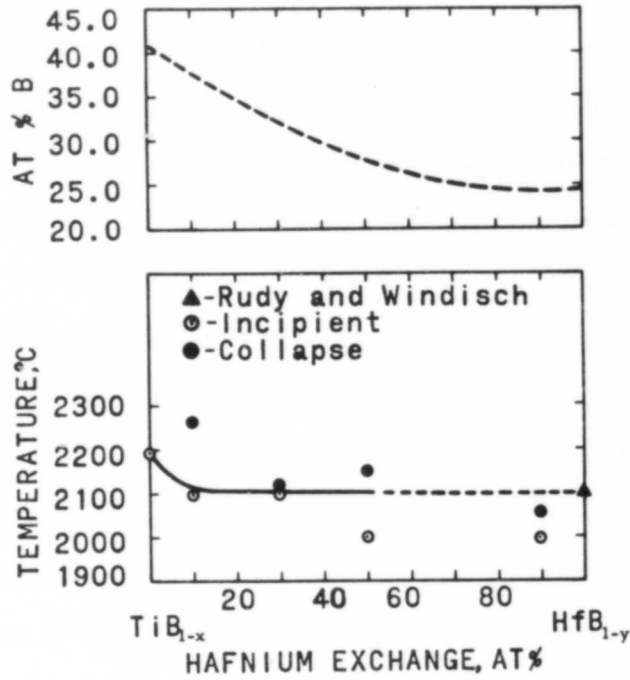


Figure 21. Composition (Top) and the Peritectic Temperatures of the Monoboride Solid Solutions.

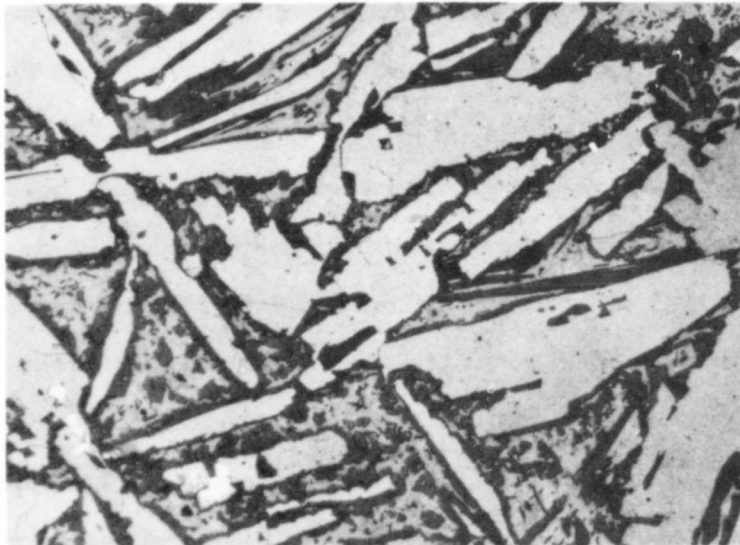


Figure 22. Micrograph of an Arc-Melted Ti-Hf-B (50/0/50) Alloy.

X250

A Non-Equilibrium Mixture of Diboride (Light), Metal (Gray) and Monoboride (Dark).

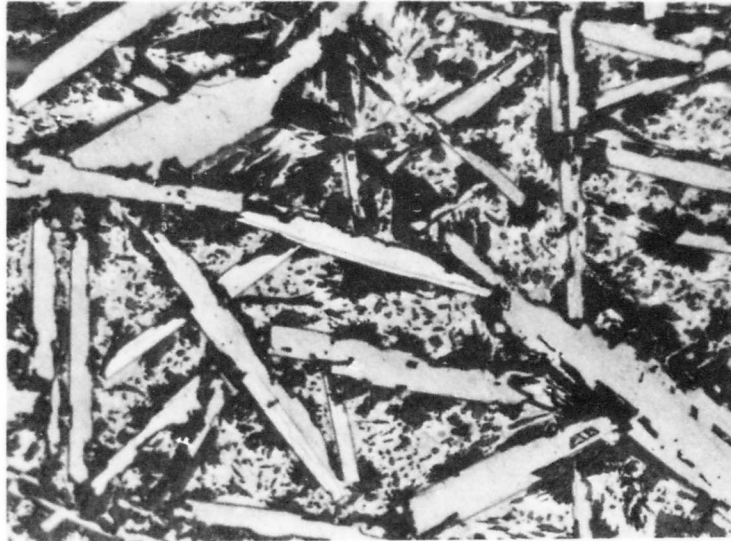


Figure 23. Micrograph of an Arc-Melted Ti-Hf-B (45/0/50) Alloy. X270

A Non-Equilibrium Mixture of Diboride (Light), Metal (Gray) and Monoboride (Dark).

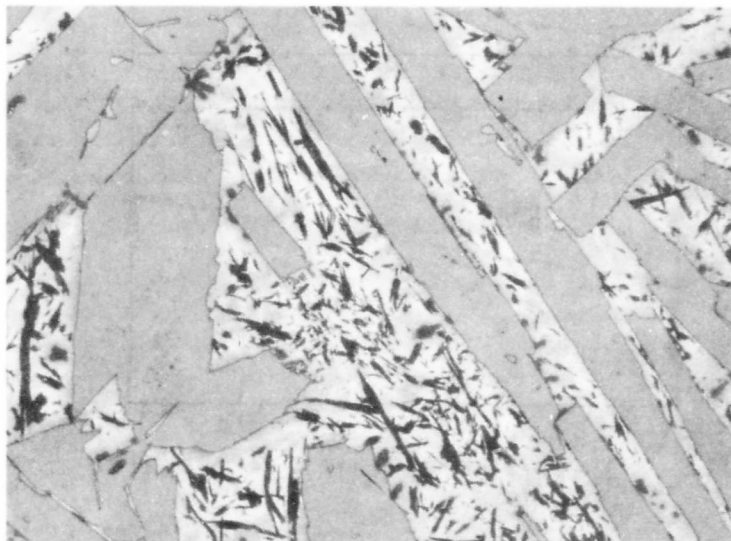


Figure 24. Micrograph of an Arc-Melted Ti-Hf-B (5/45/50) Alloy. X400

A Non-Equilibrium Mixture of Diboride (Large Gray Grains), and Monoboride (Dark Aciculan Grains) Present in the Metal Matrix.

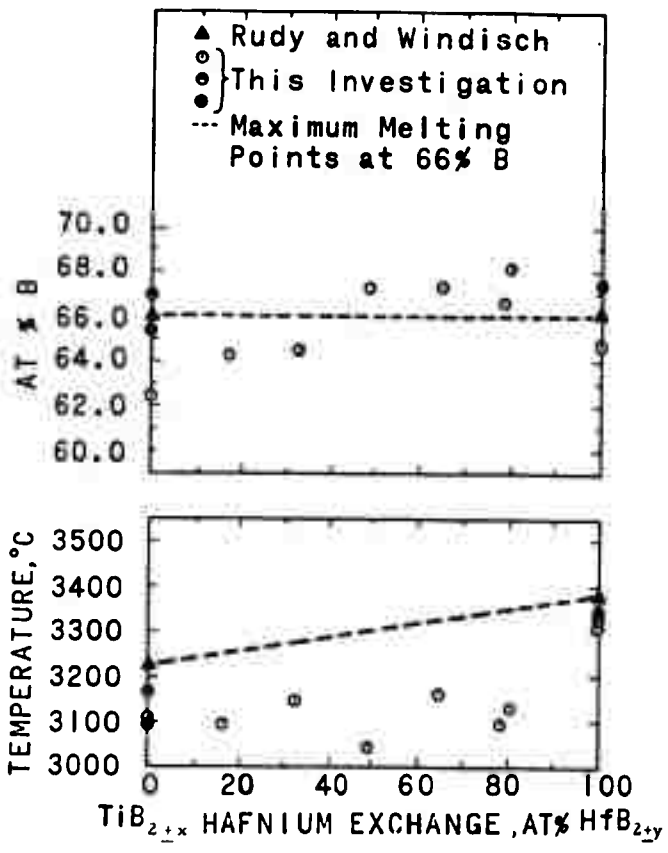


Figure 25. Composition (Top) and the Melting Temperatures of Diboride Solid Solutions.

metal-rich melt did not attack the diboride grains to form the monoboride. The monoboride (dark acicular grains) present in the metal matrix formed from the melt at temperatures below the peritectic temperature since the primary crystallization is that of the monoboride.

Some difficulty was also encountered in the determination of the melting maximum of the diboride solid solutions due to the narrow homogeneous range. The melting point drops sharply on either side of the maximum melting composition. Since the vapor pressure of boron is relatively high at the temperatures where the diboride solid solutions melt, the boron concentration in the sample depended a great deal on the history of the melting point determination. In order to determine the maximum melting point, one must measure a large number of boron-rich alloys since it was not possible to pre-determine accurately the final compositions of the alloys. After measuring the melting points of six hafnium diboride samples, the highest value obtained was 3345°C. The value of 3345°C is about 35°C lower than the highest value determined by Rudy and Windisch⁽³⁾ at a boron concentration of ~66 atomic %.

On the titanium-rich side of the diboride solid solutions, solid crystals frequently formed which blocked the black-body hole and made the melting point determination impossible. This was most probably due to the sublimation of titanium and boron simultaneously from the interior part of the black-body hole where the temperature was hotter than outside. As soon as the vapor species left the hot zone, they recombined to form diboride crystals which covered the black-body hole. These crystals were X-rayed and found indeed to be diboride.

The melting temperatures and the composition (according to chemical analysis of post-melting samples for boron content) of numerous diboride solid solutions are shown in Figure 25. The maximum melting points corresponding to about 66 atomic % boron were estimated using the binary data as a guide and are dotted in Figure 25.

A typical micrograph of one diboride solid solution, as shown in Figure 26 contains diboride with a small amount of boron at the grain boundaries.

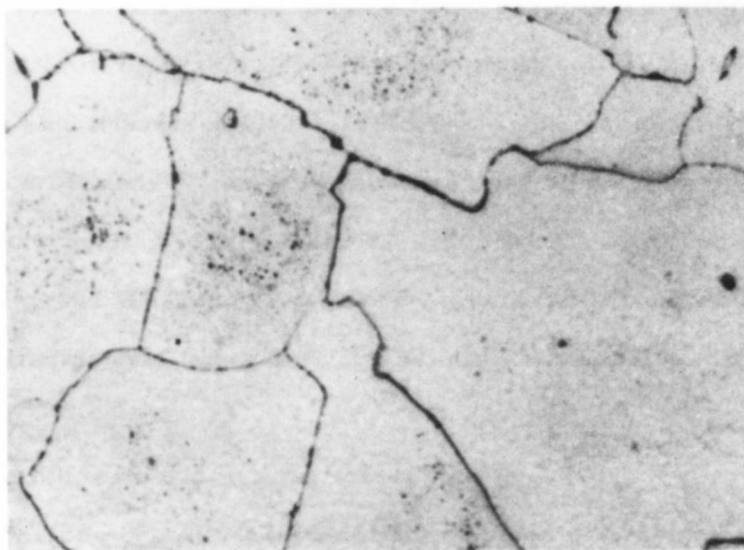
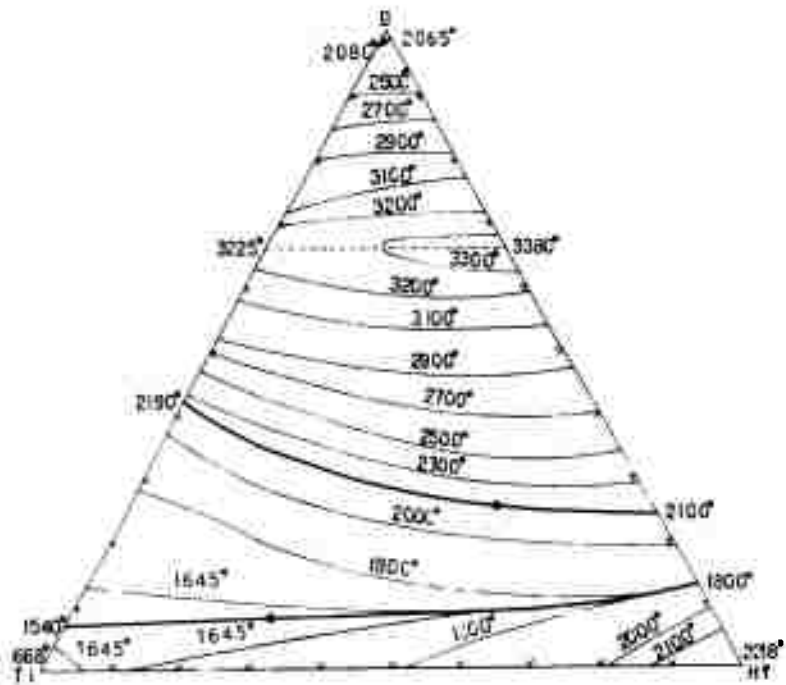


Figure 26. Micrograph of a Ti-Hf-B (16.7/16.6/66.7) Alloy. X1000
Quenched from 2700°C.

Diboride with a Small Amount of Boron at the Grain Boundaries.

The experimental evidence is summarized in the constitutional diagram titanium-hafnium-boron (Figure 2 on page 5) from 1000°C through the melting range of the diboride solid solutions. To facilitate reading of the phase diagram, the liquidus projections and a series of temperature

sections were prepared and are shown in Figures 27 through 35. The location of the tie-lines in the diboride-monoboride two-phase field were estimated, and will be discussed in detail in the discussion section. The boron-rich eutectic trough, and the course of the eutectic temperature were estimated using the binary data as a guide.



----- Maximum Solidus Temperatures of $(Ti, Hf)B_2$

Figure 27. Liquidus Projections in the Titanium-Hafnium-Boron System.

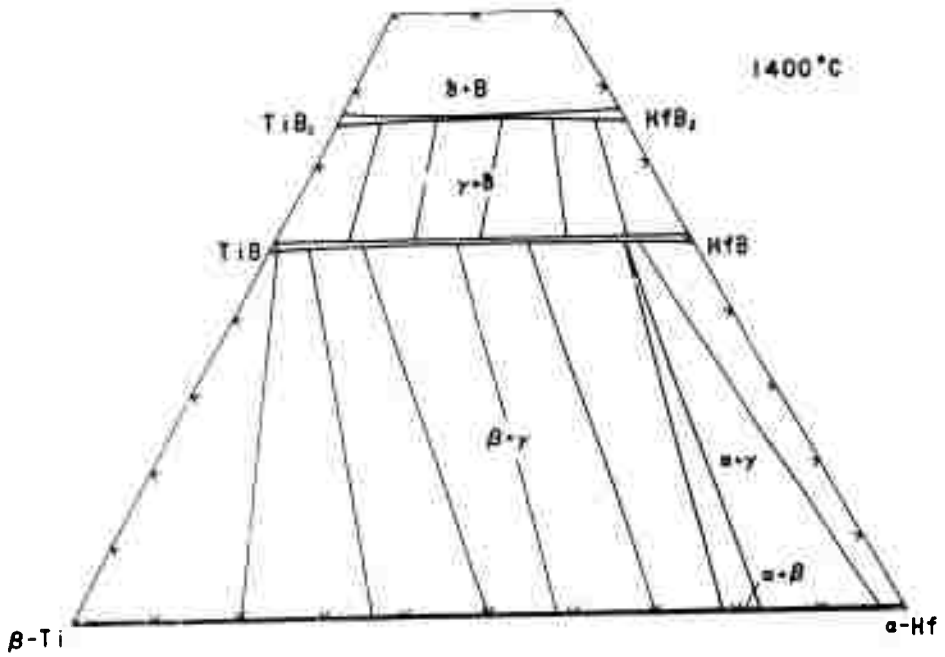


Figure 28.

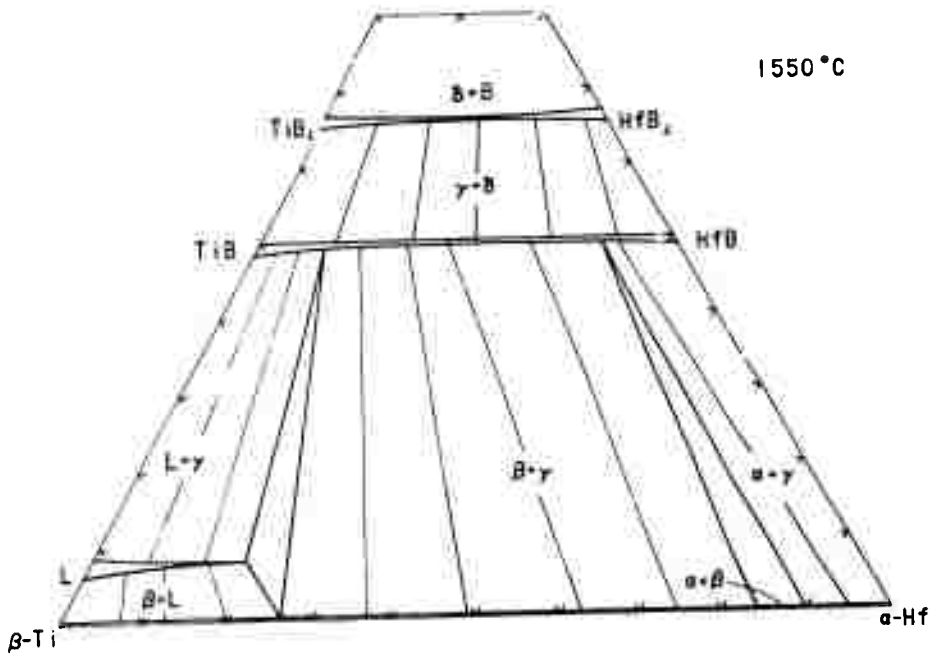


Figure 29.

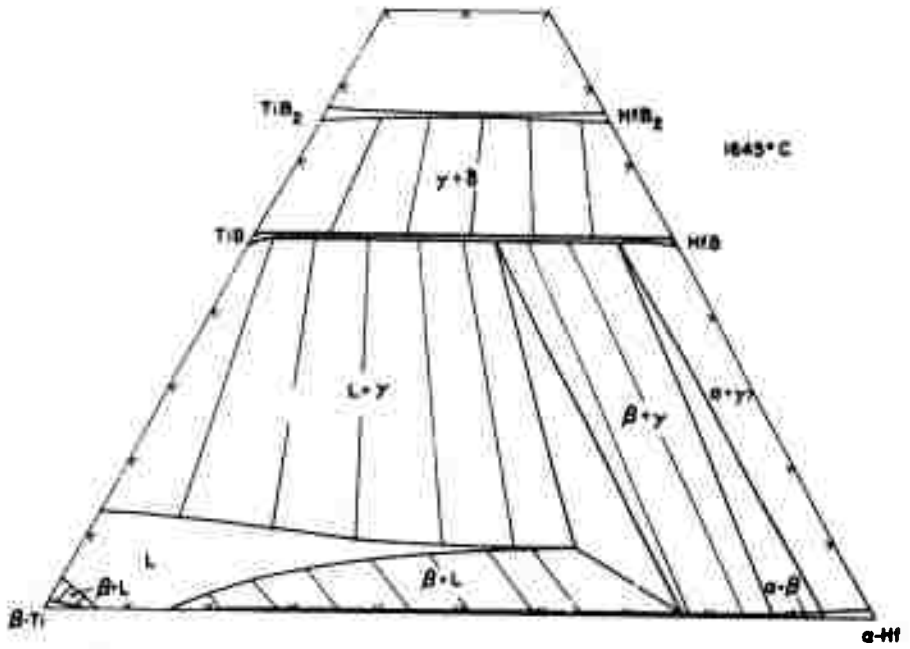


Figure 30

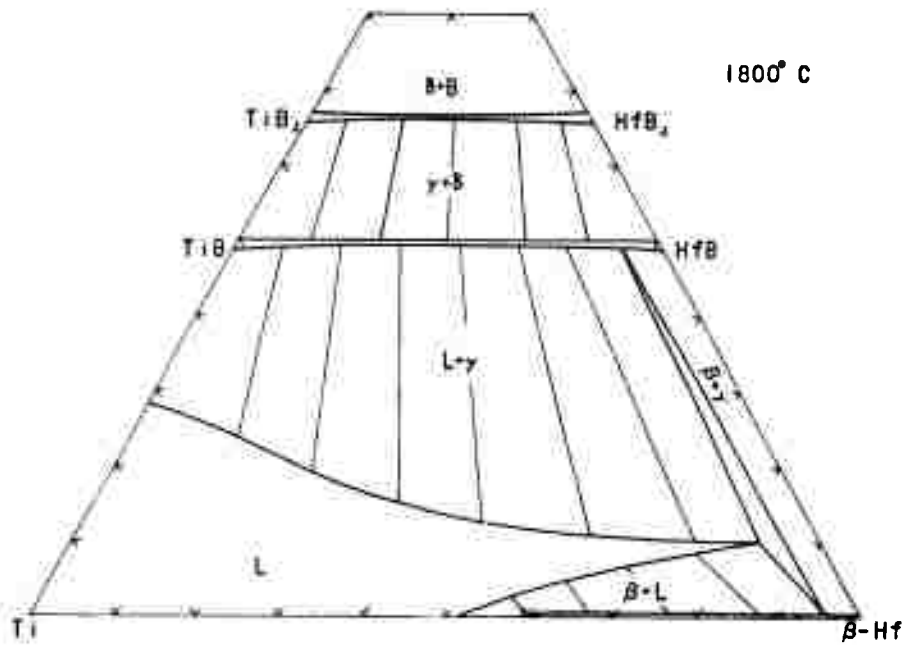


Figure 31

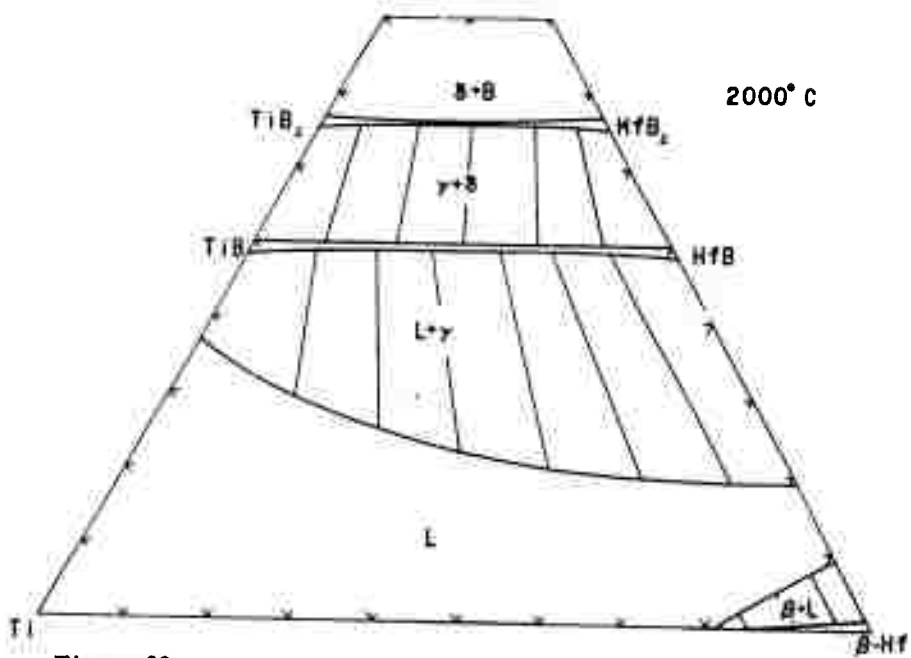


Figure 32

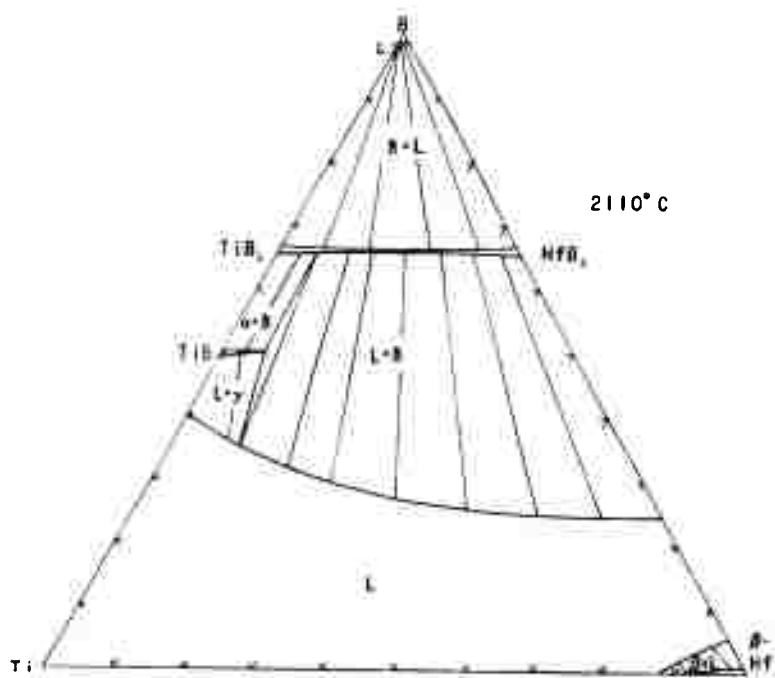


Figure 33

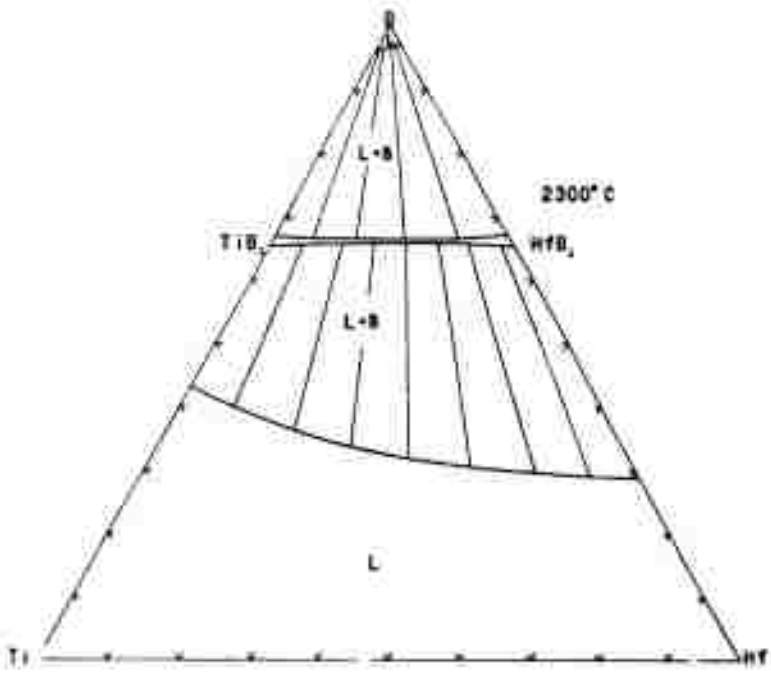


Figure 34

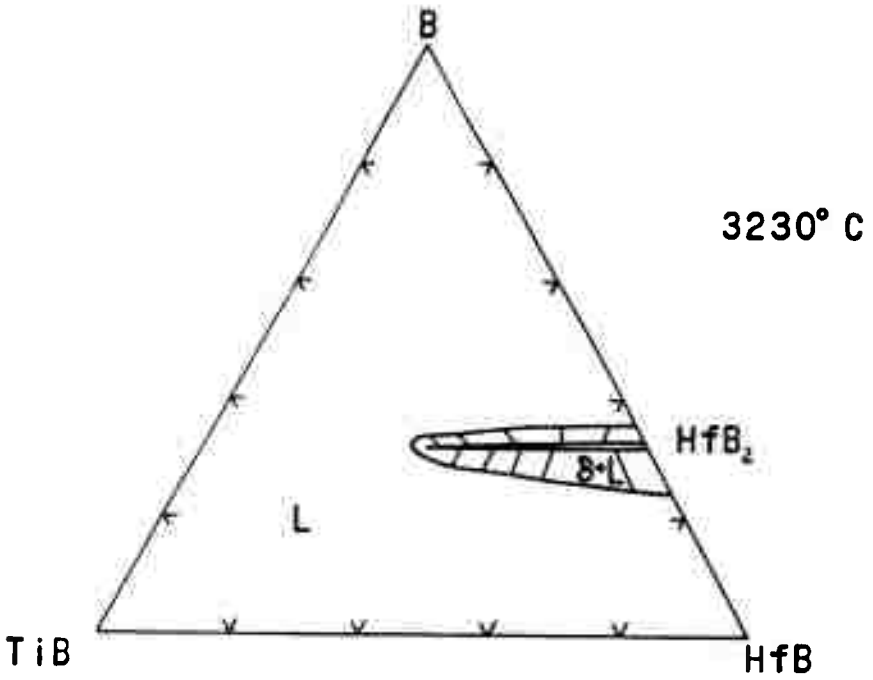


Figure 35

IV. DISCUSSION

A. PHASE EQUILIBRIA

The outstanding features of the Ti-Hf-B system at high temperatures are that both the metal diborides (δ) and the monoborides (γ) form continuous solid solutions with respect to metal exchange. The tie-lines connecting the co-existing phases in the β -metal monoboride two-phase field were established by comparing the lattice parameters of the metal phase present in the 25 atomic % boron alloys with those of the metal solutions. Although the bcc (β) structure of the titanium-rich metal solid solutions is the stable form at 1400°C, only the hcp (α) structure was found by X-ray analysis due to the extremely rapid α - β transformation. Toward the hafnium-rich side, the monoborides are in equilibrium with the α -metal solid solutions. The existence of an α - β two-phase field in the metal binary system at 1400°C results in a α - β - γ three-phase field in the ternary phase diagram.

The locations of the tie-lines in the monoboride diboride two-phase field could not be determined experimentally within a feasible length of time due to the slow formation of the monoboride solid solutions. Any alloys in the γ - δ two-phase field would contain a non-equilibrium mixture of diboride, metal solution and monoboride, since the 50 atomic % boron alloys, as already discussed earlier, never attained equilibrium even after long-time heat treatment at 1450°C.

From the locations of the tie-lines in the β - γ two-phase field, one can derive the Gibbs free energy difference, i.e. the relative stability, between the titanium monoboride and hafnium monoboride. The conditional equations governing the ternary phase equilibria have been discussed extensively by Rudy⁽¹⁾ and applied to numerous ternary metal-carbon alloy systems.^(14, 15, 16, 17, 18)

The appropriate equation for a two-phase equilibrium between two series of solid solutions with the concentrations of the third component, in the present case the boron component, being constant is,

$$\frac{\partial \Delta G^\beta}{\partial x^\beta} = \frac{\partial \Delta G^\gamma}{\partial x^\gamma} \quad (1)$$

where ΔG^β is the Gibbs free energy of formation of the bcc-metal solid solution, ΔG^γ is that of the monoboride solid solution, x^β is the mole fraction of Hf in the β -metal phase and x^γ is that of HfB in the monoboride phase. In order to obtain expressions for ΔG^β and ΔG^γ , one must know the solution behaviors for both the β -metal and monoboride solid solutions. From the shapes of the α - β and β -L phase boundaries of the binary titanium hafnium system, it is concluded that both the α -solid solutions and β -solid solutions are endothermic. Moreover, the α -solid solutions are more endothermic than the β -solid solutions. Since the regular solution approximation adequately describes the behavior of α - and β -solid solutions in the titanium-zirconium system⁽¹⁹⁾, it is reasonable to assume that the α - and β -solid solutions in the present system, titanium-hafnium also behave regularly. One additional piece of information is needed to fix the interaction parameter ϵ^a for the α -solid solutions. Using the solubility parameters given by Brewer⁽²⁰⁾ one obtains a value of about 100°K for the critical temperature of titanium-hafnium solid solutions. However, in view of the shape of the α - β phase boundaries in this system, it is more likely that the critical temperature would be somewhat higher. For lack of experimental evidence at the present, a value of 2000 cal, which corresponds to about 500°K as the critical temperature, is assumed for ϵ^a , the interaction parameter for the α -solid solution. Knowing the value of

ϵ^{α} and the α - β phase boundaries, a value of 1000 cal is obtained for ϵ^{β} , the interaction parameter for the β -solid solutions.

Assuming the monoboride solid solutions also behave regularly, the concentration gradients of ΔG^{β} and ΔG^{γ} become,

$$\frac{\partial \Delta G^{\beta}}{\partial x^{\beta}} = \Delta G_{\text{Hf}}^{\alpha-\beta} + \epsilon^{\beta} (1-2x^{\beta}) + RT \ln \frac{x^{\beta}}{1-x^{\beta}} \quad (2)$$

$$\frac{\partial \Delta G^{\gamma}}{\partial x^{\gamma}} = \Delta G_{f, \text{HfB}} - \Delta G_{f, \text{TiB}} + \epsilon^{\gamma} (1-2x^{\gamma}) + RT \ln \frac{x^{\gamma}}{1-x^{\gamma}} \quad (3)$$

From equations (1), (2), and (3), the Gibbs free energy difference between the two binary monoborides is obtained.

$$\begin{aligned} \Delta G_{f, \text{TiB}} - \Delta G_{f, \text{HfB}} &= RT \ln \frac{x^{\gamma}}{1-x^{\gamma}} \frac{1-x^{\beta}}{x^{\beta}} - \Delta G_{\text{Hf}}^{\alpha-\beta} \\ &+ \epsilon^{\gamma} (1-2x^{\gamma}) - \epsilon^{\beta} (1-2x^{\beta}) \end{aligned} \quad (4)$$

In the above equations, R is the universal constant and T is the absolute temperature. The term, $\Delta G_{\text{Hf}}^{\alpha-\beta}$ is the free energy transformation of hafnium from hcp to bcc structure and may be represented by the following equation⁽²¹⁾:

$$\Delta G_{\text{Hf}}^{\alpha-\beta} = 0.9 (2073 - T) \quad (5)$$

The assumption made in equation (5) is that $C_{p, \beta} - C_{p, \alpha} = 0$, a condition which is true to a first approximation.

In order to evaluate $\Delta G_{f, \text{TiB}} - \Delta G_{f, \text{HfB}}$ according to equation (5), one has to know the value of ϵ , the interaction parameter for the monoboride solid solutions. Different values of ϵ^{γ} varying from 0 to 3000 cal were used to calculate the Gibbs free energy difference between TiB and HfB, but a value of

2000 cal fit the experimentally determined tie-lines best (Figure 13). The value so obtained is $\Delta G_{f, TiB} - \Delta G_{f, HfB} = -2500 \pm 600$ cal. The uncertainty of 600 cal is that due to the scatter of values obtained from the individual tie lines only. However, if one also considers the uncertainties in the interaction parameters used for the various solutions, the uncertainty may be as large as ± 1000 cal. Since the tie lines in the γ - δ two-phase field were not established in the present investigations, the free energy difference between TiB_2 and HfB_2 could not be obtained.

Knowing the Gibbs free energy difference between TiB and HfB , it is now possible to calculate the phase equilibria at 1400°C between the γ -phase (monoboride) and β -phase using equations (2) and (3). The actual evaluation of the concentrations of the coexisting phases in a two-phase field is best done graphically. Since the technique has been discussed in detail by Rudy⁽¹⁴⁾, it suffices to say that the concentrations of the two respective phases in equilibrium correspond to the same concentration gradient of the Gibbs free energies, i.e. $\frac{\partial \Delta G^i}{\partial x^i} = \frac{\partial \Delta G^j}{\partial x^j}$. Similarly, the distribution of the tie lines in the γ -phase (monoboride) and α -phase (hcp phase) can be obtained utilizing the following condition,

$$\frac{\partial \Delta G^\gamma}{\partial x^\gamma} = \frac{\partial \Delta G^\alpha}{\partial x^\alpha} \quad (6)$$

The term on the right-hand side of equation (6) is

$$\frac{\partial \Delta G^\alpha}{\partial x^\alpha} = \Delta G_{Ti}^{\alpha-\beta} (1-2x^\alpha) \epsilon^\alpha + RT \ln \frac{x^\alpha}{1-x^\alpha} \quad (7)$$

The superscript α refers to the hcp-metal phase and x^α is the mole fraction of hafnium in the α -metal solution. In a manner similar to that used for hafnium, the free energy of transformation of titanium may be represented by⁽²²⁾:

$$\Delta G_{Ti}^{\alpha-\beta} = 0.88 (1155 - T) \quad (8)$$

In order to locate the three-phase field which separates the three two-phase regions: α - β , α - γ , and β - γ , one needs one additional condition, which is

$$\Delta \bar{G}_{Hf, x\alpha\beta}^{\alpha} = \Delta \bar{G}_{Hf, x\beta\alpha}^{\beta} \quad (9)$$

$$\Delta \bar{G}_{Ti, x\alpha\beta}^{\alpha} = \Delta \bar{G}_{Ti, x\beta\alpha}^{\beta} \quad (10)$$

where $\Delta \bar{G}_{Ti}$ and $\Delta \bar{G}_{Hf}$ are the relative partial molar free energies of Ti and Hf in the respective α - and β -phases, and $x\alpha\beta$ and $x\beta\alpha$ are the phase boundaries of the α -phase and β -phase in the $\alpha + \beta$ two-phase fields.

Using the well-known thermodynamic equations relating the partial molar and integral free energies, with x being mole fraction of component 2,

$$\Delta \bar{G}_{Me1} = \Delta G - x \frac{\partial \Delta G}{\partial x} \quad (11)$$

$$\Delta \bar{G}_{Me2} = \Delta G + (1-x) \frac{\partial \Delta G}{\partial x} \quad (12)$$

one obtains the following equations for the partial molar free energies of Hf in the α - and β -phases;

$$\Delta \bar{G}_{Hf}^{\alpha} = \epsilon^{\alpha} (1-x^{\alpha})^2 + RT \ln x^{\alpha} \quad (13)$$

$$\Delta \bar{G}_{Hf}^{\beta} = \Delta G_{Hf}^{\alpha-\beta} + \epsilon^{\beta} (1-x^{\beta})^2 + RT \ln x^{\beta} \quad (14)$$

The numerical evaluation for the values of $x\alpha\beta$ and $x\beta\alpha$ is best done by picking out the values of x^{α} and x^{β} from the Gibbs free energy gradient curves ($\frac{\partial \Delta G^i}{\partial x^i}$ vs x^i curves), and substituting these values in equations (13) and (14).

By plotting these values so obtained for $\Delta\bar{G}_{Hf}^{\alpha} - \Delta\bar{G}_{Hf}^{\beta}$ as a function of either x^{α} or x^{β} , the values of $x_{\alpha\beta}$ and $x_{\beta\alpha}$ when $\Delta\bar{G}_{Hf}^{\alpha} - \Delta\bar{G}_{Hf}^{\beta} = 0$ (equation 9) are obtained.

The calculated phase diagram at 1400°C as shown in Figure 36 is in reasonable agreement with the actual phase diagram (Figure 13).

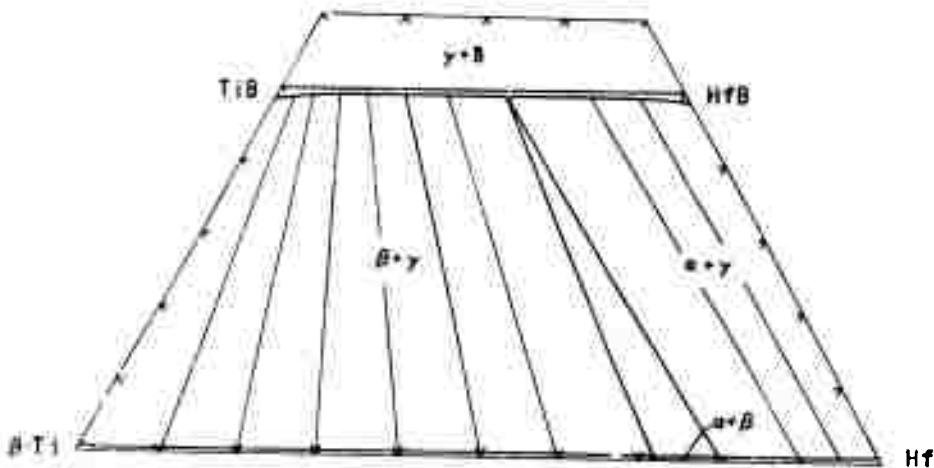


Figure 36. Calculated Phase Diagram at 1400°C for Titanium-Hafnium-Boron System.

The distribution of the calculated tie-lines is more self-consistent than that of the experimentally determined ones since the value of $\Delta G_{f, TiB} - \Delta G_{f, HfB} = -2500 + 600 \text{ cal/g. atom metal}$ is an average value obtained from the individual tie-lines.

In order to calculate the tie-line distribution in the γ - δ two-phase field, it is necessary to know the Gibbs free energy difference between TiB_2 and HfB_2 in addition to the Gibbs free energy difference between TiB and HfB as shown by the following equation:

$$RT \ln \frac{x^\delta}{1-x^\delta} - \frac{1-x^\gamma}{x^\gamma} = (\Delta G_{f, HfB} - \Delta G_{f, TiB}) - (\Delta G_{f, HfB_2} - \Delta G_{f, TiB_2}) \quad (15)$$

In the above equation, x^δ is the mole fraction of HfB_2 in the diboride solid solution, x^γ is the mole fraction of HfB in the monoboride solid solution, and $\Delta G_{f, HfB_2}$ and $\Delta G_{f, TiB_2}$ are the Gibbs free energies of formation of HfB_2 and TiB_2 , respectively. From the recent phase investigations of the ternary systems Zr-Hf-B and Ti-Zr-B at 1400°C by Harmon⁽²³⁾ and Eckert⁽²⁴⁾, HfB_2 was found to be much more stable than TiB_2 . This result is in accord with the thermodynamic data available in the literature⁽²⁵⁾. Based on these data, the tie lines in the γ - δ two-phase field as shown in Figures 28 through 35 were drawn with inclinations toward HfB_2 side.

B. APPLICATION

Due to the inherent brittleness of the otherwise oxidation-resistant diborides, one must utilize composite systems consisting of primary diboride matrix with metal constituents in order to overcome the thermal shock problem. Although the monoboride solid solutions existing in the titanium-hafnium-boron system are thermodynamically stable, the formation of the hafnium-rich monoboride solid solution is rarely complete even after the alloys are heat-treated for 300 hours at 1450°C. Rudy and Windisch⁽³⁾

THIS REPORT HAS BEEN DELIMITED
AND CLEARED FOR PUBLIC RELEASE
UNDER DOD DIRECTIVE 5200.20 AND
NO RESTRICTIONS ARE IMPOSED UPON
ITS USE AND DISCLOSURE.

DISTRIBUTION STATEMENT A
APPROVED FOR PUBLIC RELEASE,
DISTRIBUTION UNLIMITED.

have quenched a mixture of hafnium diboride and hafnium with a gross composition around 50 atomic % boron from high temperature followed by long time heat treatment at 1400°C. They found virtually no back reaction between diboride and metal to form the monoboride. In view of the sluggishness of the reaction between the diboride and metal to form the stable monoboride at the hafnium-rich side, one can still prepare a metastable diboride-metal composite for services below the metal-rich eutectic temperatures.

REFERENCES

1. E. Rudy: *Z. Metallkde.*, 54, 213 (1963).
2. E. Rudy and St. Windisch: AFML-TR-65-2, Part I, Vol VII, (October 1965).
3. E. Rudy and St. Windisch: AFML-TR-65-2, Part I, Vol. IX, (October 1965).
4. E. T. Hayes and D.K. Deardorff: Work quoted in the Metallurgy of Hafnium, edited by D.E. Thomas and E.T. Hayes, Naval Reactors Division of Reactor Development, United States Atomic Energy Commission (1960).
5. M.Hansen and K. Anderko: *Constitution of Binary Alloys*, 2nd Edition, McGraw-Hill, New York (1958).
6. B. Post, F.W. Glaser and D. Moskowitz: *Acta Met.* 2, 20 (1954).
7. K.C. Antony and W.V. Cummings, GEAP 3530 (1960).
8. E. Rudy, St. Windisch and Y.A. Chang: AFML-TR-65-2, Part I Vol. I (1965).
9. H.D. Heetderks, E. Rudy and T.E. Eckert: AFML-TR-65-2, Part IV, Vol. I (1965).
10. B.D. Cullity: *Elements of X-ray Diffraction*, Addison-Wesley Publishing Company, Inc., Reading, Massachusetts, (1956).
11. R.B. Russell, *J. Appl. Phys.*, 24 232 (1953).
12. B.F. Decker and J.S. Kasper, *Acta. Cryst.* 7, 77 (1954).
13. E. Rudy and F. Benesovsky, *Monat. Chem.*, 92, 415 (1961).
14. E. Rudy: *Z. Metallk.*, 54 213 (1963).
15. E. Rudy, *Thermodynamics of Nuclear Materials*, International Atomic Energy Agency, Vienna (1962).
16. E. Rudy and H. Nowotny: *Monat. Chem.*, 94 507 (1963).
17. E. Rudy and Y.A. Chang: *Plansee Proceedings, 1964*. Edited by F. Benesovsky, Metallwerk Plansee, A.G., Reutte, Tirol, 786 (1965).
18. D.P. Harmon and C.E. Brukl: AFML-TR-65-2, Part I, Vol. IV (1965).
19. L. Kaufman, *Acta. Met.*, 1, 575 (1959).

References (Continued)

20. L. Brewer: "Prediction of High Temperature Metallic Phase Diagrams in High-Strength Materials", Edited by V.F. Zackay, John Wiley & Sons, Inc., New York (1965).
21. Y.A. Chang: AFML-TR-65-2, Part IV, Vol. I (1965).
22. R. Hultgren, R.L. Orr, P.D. Anderson and K.K. Kelley: Selected Values of Thermodynamic Properties of Metals and Alloys, John Wiley and Sons, Inc., New York (1963).
23. D.P. Harmon: Part II, Volume VI, AFML-TR-65-2 (1965) Contract AF 33(615)-1249.
24. T.E. Eckert: Part II, Volume XII, AFML-TR-65-2 (1965) Contract AF 33(615)-1249.
25. L. Kaufman: Compounds of Interest in Nuclear Technology, Edited by J.T. Waber, P. Chiotti and W.N. Miner, 193 (1964.)

DOCUMENT CONTROL DATA - R&D		
<small>(Security classification of title, body of abstract and indexing annotation must be entered when the overall report is classified)</small>		
1 ORIGINATING ACTIVITY (Corporate author) Materials Research Laboratory Aerojet-General Corporation Sacramento, California		2a REPORT SECURITY CLASSIFICATION Unclassified
		2b GROUP N.A.
3 REPORT TITLE Ternary Phase Equilibria in Transition Metal-Boron-Carbon-Silicon Systems Part II. Ternary Systems. Volume V. Ti-Hf-B System		
4 DESCRIPTIVE NOTES (Type of report and inclusive dates) Documentary Report		
5 AUTHOR(S) (Last name, first name, initial) Y. A. Chang		
6 REPORT DATE March 1966	7a. TOTAL NO. OF PAGES 51	7b. NO. OF REFS 25
8a. CONTRACT OR GRANT NO. AF 33(615)-1249	8a. ORIGINATOR'S REPORT NUMBER(S) AFML-TR-65-2 Part II, Volume V	
b. PROJECT NO. 7350		
c. Task No. 735001	8b. OTHER REPORT NO(S) (Any other numbers that may be assigned this report) N.A.	
d.		
10 AVAILABILITY/LIMITATION NOTICES : This document is subject to special export controls and each transmittal to foreign governments or foreign nationals may be made only with prior approval of Metals & Ceramics Div., AF Materials Laboratory, Wright-Patterson AFB, Ohio.		
11 SUPPLEMENTARY NOTES	12. SPONSORING MILITARY ACTIVITY AFML (MAMC) Wright-Patterson AFB, Ohio, 45433	
13 ABSTRACT ↓ A complete phase diagram for the ternary alloy system titanium-hafnium-boron from 1000°C through the melting ranges of the diborides was established on the basis of X-ray, melting point and metallographic studies. The outstanding features of the system are that both the metal diborides and monoborides form continuous solid solutions with respect to metal exchange. From the distribution of the tie-lines in the metal monoboride two-phase field, the Gibbs free energy difference between the titanium monoboride and hafnium monoboride was derived. ↑		

14	KEY WORDS	LINK A		LINK B		LINK C	
		ROLE	WT	ROLE	WT	ROLE	WT
High Temperature Phase Equilibrium Borides							

INSTRUCTIONS

1. **ORIGINATING ACTIVITY:** Enter the name and address of the contractor, subcontractor, grantee, Department of Defense activity or other organization (*corporate author*) issuing the report.

2a. **REPORT SECURITY CLASSIFICATION:** Enter the overall security classification of the report. Indicate whether "Restricted Data" is included. Marking is to be in accordance with appropriate security regulations.

2b. **GROUP:** Automatic downgrading is specified in DoD Directive 5200.10 and Armed Forces Industrial Manual. Enter the group number. Also, when applicable, show that optional markings have been used for Group 3 and Group 4 as authorized.

3. **REPORT TITLE:** Enter the complete report title in all capital letters. Titles in all cases should be unclassified. If a meaningful title cannot be selected without classification, show title classification in all capitals in parenthesis immediately following the title.

4. **DESCRIPITIVE NOTES:** If appropriate, enter the type of report, e.g., interim, progress, summary, annual, or final. Give the inclusive dates when a specific reporting period is covered.

5. **AUTHOR(S):** Enter the name(s) of author(s) as shown on or in the report. Enter last name, first name, middle initial. If military, show rank and branch of service. The name of the principal author is an absolute minimum requirement.

6. **REPORT DATE:** Enter the date of the report as day, month, year, or month, year. If more than one date appears on the report, use date of publication.

7a. **TOTAL NUMBER OF PAGES:** The total page count should follow normal pagination procedures, i.e., enter the number of pages containing information.

7b. **NUMBER OF REFERENCES:** Enter the total number of references cited in the report.

8a. **CONTRACT OR GRANT NUMBER:** If appropriate, enter the applicable number of the contract or grant under which the report was written.

8b, 8c, & 8d. **PROJECT NUMBER:** Enter the appropriate military department identification, such as project number, subproject number, system numbers, task number, etc.

9a. **ORIGINATOR'S REPORT NUMBER(S):** Enter the official report number by which the document will be identified and controlled by the originating activity. This number must be unique to this report.

9b. **OTHER REPORT NUMBER(S):** If the report has been assigned any other report numbers (*other by the originator or by the sponsor*), also enter this number(s).

10. **AVAILABILITY/LIMITATION NOTICES:** Enter any limitations on further dissemination of the report, other than those

imposed by security classification, using standard statements such as:

- (1) "Qualified requesters may obtain copies of this report from DDC."
- (2) "Foreign announcement and dissemination of this report by DDC is not authorized."
- (3) "U. S. Government agencies may obtain copies of this report directly from DDC. Other qualified DDC users shall request through _____."
- (4) "U. S. military agencies may obtain copies of this report directly from DDC. Other qualified users shall request through _____."
- (5) "All distribution of this report is controlled. Qualified DDC users shall request through _____."

If the report has been furnished to the Office of Technical Services, Department of Commerce, for sale to the public, indicate this fact and enter the price, if known.

11. **SUPPLEMENTARY NOTES:** Use for additional explanatory notes.

12. **SPONSORING MILITARY ACTIVITY:** Enter the name of the departmental project office or laboratory sponsoring (*or performing for*) the research and development. Include address.

13. **ABSTRACT:** Enter an abstract giving a brief and factual summary of the document indicative of the report, even though it may also appear elsewhere in the body of the technical report. If additional space is required, a continuation sheet shall be attached.

It is highly desirable that the abstract of classified reports be unclassified. Each paragraph of the abstract shall end with an indication of the military security classification of the information in the paragraph, represented as (TS), (S), (C), or (U).

There is no limitation on the length of the abstract. However, the suggested length is from 150 to 225 words.

14. **KEY WORDS:** Key words are technically meaningful terms or short phrases that characterize a report and may be used as index entries for cataloging the report. Key words must be selected so that no security classification is required. Identifiers, such as equipment model designation, trade name, military project code name, geographic location, may be used as key words but will be followed by an indication of technical context. The assignment of links, rules, and weights is optional.